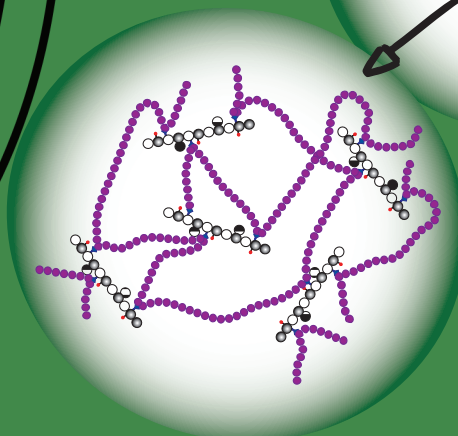
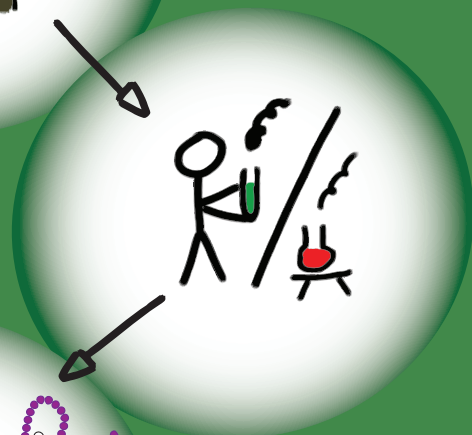


Chemical Derivatization of Galactoglucomannan for Functional Materials

Daniel Dax



Laboratory of Wood and Paper Chemistry
Process Chemistry Centre
Department of Chemical Engineering
Åbo Akademi University
Turku/Åbo 2014

Chemical Derivatization of Galactoglucomannan for Functional Materials

Daniel Dax



Laboratory of Wood and Paper Chemistry
Process Chemistry Centre
Department of Chemical Engineering
Åbo Akademi University

Turku/Åbo 2014

Daniel Dax

Born in Luxembourg 1984

Diplom-Chemiker 2010,
RWTH Aachen University, Germany



Fonds National de la
Recherche Luxembourg

Supported by the Fonds National de la Recherche, Luxembourg (1000030)

Supervised by

Professor Stefan Willför

and

Docent Dr. Chunlin Xu
Laboratory of Wood and Paper Chemistry
Process Chemistry Centre
Åbo Akademi University
Turku/Åbo, Finland

Reviewers

Professor Maija Tenkanen
Department of Food and Environmental Sciences
University of Helsinki
Helsinki, Finland

Associate Professor Ulrica Edlund
Fibre and Polymer Technology
Royal Institute of Technology
Stockholm, Sweden

Opponent

Associate Professor Ulrica Edlund

Custos

Professor Stefan Willför

ISBN: 978-952-12-3115-5

Contents

PREFACE.....	iv
ABSTRACT	v
LIST OF PUBLICATIONS.....	ix
SUPPORTING PUBLICATIONS.....	x
1. INTRODUCTION.....	1
2. AIMS AND OBJECTIVES OF THIS STUDY.....	2
3. BACKGROUND.....	3
3.1 Polysaccharides.....	3
3.2 O-acetyl galactoglucomannan (GGM)	5
3.3 Nanofibrillated cellulose (NFC).....	7
3.4 Chemical modifications of polysaccharides.....	7
3.4.1 Esterification, etherification, and oxidation of polysaccharides.....	9
3.4.2 Reactions of the reducing end group of polysaccharides	10
3.4.3 Polymerization	10
3.5 Application of chemically modified polysaccharides.....	13
4. EXPERIMENTAL	15
4.1 Materials	15
4.2 Methods.....	16
4.2.1 High Performance Size Exclusion Chromatography (HPSEC) [I-IV]	16
4.2.2 Nuclear Magnetic Resonance spectroscopy (NMR) [I-IV].....	16
4.2.3 Calibration of the ¹ H NMR spectra	17
4.2.4 Fourier Transformed Infrared Spectroscopy (FTIR) [I-IV].....	18
4.2.5 Thermal Gravimetric Analysis (TGA) [I, II].....	18
4.2.6 Quartz Crystal Microbalance with Dissipation Monitoring (QCM-D) [III]	18
4.2.7 Oxygen Transmission Rate (OTR) [III].....	19
4.2.8 Water Contact Angle (CA) [III].....	19

4.2.9	Determination of the surface tension in water [I, III].....	19
4.2.10	Determination of the Area (A) occupied by the adsorbed molecules at the water-air interface.....	19
4.2.11	Swelling of the GGM-based hydrogels [IV].....	20
4.3	Synthesis.....	20
4.3.1	Synthesis of Me ₆ -TREN [II].....	20
4.3.2	Preparation of tert-butyl-N-(2-aminoethyl) carbonate (NH ₂ -BOC) [I, II].....	21
4.3.3	Amidation of α-bromoisobutyryl bromide (BIBB) with NH ₂ -BOC [II].....	21
4.3.4	Synthesis of the GGM macroinitiator [II].....	22
4.3.5	SET-LRP using the GGM macroinitiator [II].....	22
4.3.6	Activation of the fatty acids [I].....	23
4.3.7	Amidation of the activated fatty acids with NH ₂ -BOC [I].....	23
4.3.8	Esterification of GGM with activated fatty acids [I].....	23
4.3.9	Reductive amination of GGM using amino functional fatty acids [I].....	24
4.3.10	Synthesis of GGM-block-PDMS [III].....	24
4.3.11	Synthesis of GGM-MA macromonomers [IV].....	24
4.3.12	Synthesis of the GGM-based hydrogels [IV].....	25
5.	RESULTS AND DISCUSSION.....	26
5.1	Overview of the experiments.....	26
5.2	Synthesis of GGM derivatives.....	28
5.2.1	Amphiphilic GGM-fatty acid derivatives [I].....	28
5.2.2	Block-copolymers of GGM and PDMS [III].....	37
5.2.3	Functional GGM-block-structured derivatives by SET-LRP [II].....	42
5.2.4	GGM-based hydrogels [IV].....	47
5.3	Physical characterization and applications of the GGM derivatives.....	53
5.3.1	Reduction of surface tension in water by GGM-fatty acid derivatives [I].....	53
5.3.2	Modification of cellulosic surfaces by amphiphilic GGM derivatives [III].....	55

5.3.3 Metal ion removal from aqueous solution using GGM-based hydrogels [IV]	58
6. CONCLUDING REMARKS.....	62
NOTATIONS.....	64
REFERENCES.....	66

PREFACE

The present work was carried in the framework of the Process Chemistry Centre in the Laboratory of Wood and Paper Chemistry, Department of Chemical Engineering at the Åbo Akademi University between November 2010 and November 2014.

First and foremost, I am expressing my sincere gratitude to Professor Stefan Willför for giving me the opportunity to carry out an interesting research at his laboratory. I am most grateful for his supervision along my work and for his support for the development of new ideas. To Docent Dr. Chunlin Xu I want to express my deepest appreciation for this help along my work, the constructive and inspiring discussion, together with his patience during more turbulent days. Furthermore, I want to thank Professor Regis Teixeira Mendonça for giving me the possibility to perform part of my work in his laboratory. Also, Dr. Julio Sánchez is thanked for the interesting and fruitful discussions and co-operation.

I would like to thank Docent Dr. Anna Sundberg for her kind advices and for helping me with the Swedish translation of the abstract. I want to express my gratitude to Leif Österholm for helping me in many cases and making the laboratory work most efficient. Also Jarl Hemming and Dr. Hanna Lindqvist are thanked for being always helpful in different situations. I would like to thank all the co-authors and co-workers for the successful collaboration.

Thank you to all my friends for your priceless support and encouragement.

My deepest gratitude I want to address to my family; my mother, my father, and my two brothers, Pol and Claude, for their invaluable support and motivation along my thesis work. Special thanks also to Daniel for being an irreplaceable friend over decades. Last but not least, many thanks to Camila for always supporting me and for her patience.

ABSTRACT

Daniel Dax

“Chemical Derivatization of Galactoglucomannan for Functional Materials”

Doctoral Thesis, Laboratory of Wood and Paper Chemistry, Process Chemistry Centre, Department of Chemical Engineering, Åbo Akademi University, 2014.

Keywords: Biorefinery, hemicelluloses, *O*-acetyl galactoglucomannan, reductive amination, esterification, transesterification, surfactant, hydrogel, single electron transfer-living radical polymerization.

In the framework of the biorefinery concept researchers aspire to optimize the utilization of plant materials, such as agricultural wastes and wood. For most of the known processes, the first steps in the valorisation of biomass are the extraction and purification of the individual components. The obtained raw products by means of a controlled separation can consecutively be modified to result in biofuels or biogas for energy production, but also in value-added products such as additives and important building blocks for the chemical and material industries. Considerable efforts are undertaken in order to substitute the use of oil-based starting materials or at least minimize their processing for the production of everyday goods. Wood is one of the raw materials, which have gained large attention in the last decades and its composition has been studied in detail. Nowadays, the extraction of water-soluble hemicelluloses from wood is well known and so for example xylan can be obtained from hardwoods and *O*-acetyl galactoglucomannans (GGMs) from softwoods. The aim of this work was to develop water-soluble amphiphilic materials of GGM and to assess their potential use as additives. Furthermore, GGM was also applied as a crosslinker in the synthesis of functional hydrogels for the removal of toxic metals and metalloids ions from aqueous solutions. The distinguished products were obtained by several chemical approaches and analysed by nuclear magnetic resonance spectroscopy (NMR), Fourier transform infrared spectroscopy (FTIR), size exclusion chromatography (SEC), thermal gravimetric analysis (TGA), scanning electron microscope SEM, among others.

Bio-based surfactants were produced by applying GGM and different fatty acids as starting materials. On one hand, GGM-grafted-fatty acids were prepared by esterification and on the other hand, well-defined GGM-block-fatty acid derivatives were obtained by linking amino-functional fatty acids to the reducing end of GGM. The

reaction conditions for the syntheses were optimized and the resultant amphiphilic GGM derivatives were evaluated concerning their ability to reduce the surface tension of water as surfactants. Furthermore, the block-structured derivatives were tested in respect to their applicability as additives for the surface modification of cellulosic materials. Besides the GGM surfactants with a bio-based hydrophilic and a bio-based hydrophobic part, also GGM block-structured derivatives with a synthetic hydrophobic tail, consisting of a polydimethylsiloxane chain, were prepared and assessed for the hydrophobization of surface of nanofibrillated cellulose films.

In order to generate GGM block-structured derivatives containing a synthetic tail with distinguished physical and chemical properties, as well as a tailored chain length, a controlled polymerization method was used. Therefore, firstly an initiator group was introduced at the reducing end of the GGM and consecutively single electron transfer-living radical polymerization (SET-LRP) was performed by applying three different monomers in individual reactions. For the accomplishment of the synthesis and the analysis of the products, challenges related to the solubility of the reactants had to be overcome. Overall, a synthesis route for the production of GGM block-copolymers bearing different synthetic polymer chains was developed and several derivatives were obtained.

Moreover, GGM with different molar masses were, after modification, used as a crosslinker in the synthesis of functional hydrogels. Hereby, a cationic monomer was used during the free radical polymerization and the resultant hydrogels were successfully tested for the removal of chromium and arsenic ions from aqueous solutions. The hydrogel synthesis was tailored and materials with distinguished physical properties, such as the swelling rate, were obtained after purification. The results generated in this work underline the potential of bio-based products and the urge to continue carrying out research in order to be able to use more green chemicals for the manufacturing of biorenewable and biodegradable daily products.

Sammanfattning

Inom konceptet för bioraffinering försöker forskarna optimera användningen av växter, såsom jordbruksavfall och ved. I de flesta kända metoderna, som siktar på att tillvarata värdefulla komponenter, är det första steget extraktion och rening av biomassans komponenter. Produkterna som fås genom en kontrollerad separation av råmaterialet kan vidare modifieras till biobränslen eller biogas för energiproduktion, men också till produkter med mervärde, såsom tillsatsmedel och viktiga byggstenar för den kemiska industrin. Avsevärda ansträngningar har gjorts för att ersätta, eller åtminstone minimera, oljebaserade råmaterial i produktionen av dagligvaror. Trä är en av de råvaror som har fått stor uppmärksamhet under det senaste decenniet och dess sammansättning har studerats i detalj. Numera är utvinning av vattenlösliga hemicelluloser från ved noggrant studerad och till exempel kan xylaner utvinnas från lövträd och O-acetylgalaktoylglukomannaner (GGM) från barrved. Syftet med detta arbete var att bedöma lämpligheten av GGM som material för utveckling av vattenlösliga amfifila material och vidare hur dessa material kunde användas som tillsatsmedel. Dessutom användes GGM som en tvärbindare vid syntes av funktionella hydrogeler som kan användas för att avlägsna giftiga metaller och halvmetalljoner från vattenbaserade lösningar. Produkterna framställdes med hjälp av olika kemiska metoder och analyserades med t.ex. kärnmagnetisk resonans (NMR), fouriertransformerad infrarödspektroskopi (eng. Fourier transform infrared spectroscopy, FTIR), storlekskromatografi (SEC), termogravimetrisk analys (TGA) och svepelektronmikroskopi (SEM).

I detta arbete producerades biobaserade ytaktiva ämnen baserade på GGM och olika fettsyror som utgångsmaterial. Å ena sidan framställes GGM-ympade fettsyror genom förestringsreaktioner, och å andra sidan erhöles ett väldefinierat GGM-block-fettsyraderivat genom att länka aminofunktionella fettsyror till den reducerande änden av GGM. Reaktionsbetingelserna för syntesen optimerades och de erhållna amfifila GGM-derivaten utvärderades med avseende på deras förmåga att reducera vattnets ytspänning. Vidare undersöktes segmentstrukturderivaten som tillsatser för ytbearbetning av cellulosa. Förutom ytaktiva ämnen av GGM, med en biobaserad hydrofil och en biobaserad hydrofob del, framställdes och testades även ett GGM-block-strukturderivat med en syntetisk hydrofob svans bestående av en poly(dimethylsiloxane)-kedja med avseende på hydrofobisering av nanofibrillerad cellulosa.

För att framställa GGM-block-strukturderivat med en syntetisk svans med specifika fysikaliska och kemiska egenskaper samt en skräddarsydd kedjelängd, användes en kontrollerad polymerisationsmetod. Först inympades en initiator vid den reducerande änden av GGM, följt av en aktiv radikalpolymerisation med singel elektronöverföring med tre olika monomerer. För att möjliggöra syntes och kunna analysera produkterna, måste utmaningar med reaktanternas löslighet övervinnas. Sammanfattningsvis har en syntesväg för framställning av GGM-segmentsampolymerer med olika syntetiska polymerkedjor utvecklats och flera derivat erhållits.

Ett annat område där polysackarider har använts är hydrogeler. I detta arbete användes modifierad GGM med olika molmassor, som en tvärbindare vid syntes av funktionella hydrogeler. Då en katjonisk monomer användes under polymerisation med fria radikaler, kunde krom (Cr) och arsenik (As) framgångsrikt avlägsnas från vattenlösningar. Hydrogelsyntesen kunde skräddarsys och material med framstående fysikaliska egenskaper, såsom potentiell vattenupptagning, erhöles efter rening. De resultat som genererats i detta arbete understryker potentialen för biobaserade produkter och nödvändigheten att fortsätta med forskning för att kunna använda fler gröna kemikalier vid tillverkning av bioförnybara och biologiskt nedbrytbara dagligvaror.

LIST OF PUBLICATIONS

- I. Dax, D.; Eklund, P.; Hemming, J.; Sarfraz, J.; Backman, P.; Xu, C.; Willför, S., Amphiphilic spruce galactoglucomannan derivatives based on naturally-occurring fatty acids. *Bioresources* **2013**, 8 (3), 3771-3790.
- II. Dax, D.; Xu, C.; Långvik, O.; Hemming, J.; Backman, P.; Willför, S., Synthesis of SET-LRP-induced galactoglucomannan-diblock copolymers. *Journal of Polymer Science Part A: Polymer Chemistry* **2013**, 51 (23), 5100-5110.
- III. Lozhechnikova, A.; Dax, D.; Vartiainen, J.; Willför, S.; Xu, C.; Österberg, M., Modification of nanofibrillated cellulose using amphiphilic block-structured galactoglucomannans. *Carbohydrate Polymers* **2014**, 110, 163 - 172.
- IV. Dax, D.; Chávez, M. S.; Xu, C.; Willför, S.; Mendonça, R. T.; Sánchez, J., Cationic hemicellulose-based hydrogels for arsenic and chromium removal from aqueous solutions. *Carbohydrate Polymers* **2014**, 111, 797-805.

CONTRIBUTION OF THE AUTHOR

For the publications [I] and [II] the author of the thesis developed the synthesis route, performed, all the synthesis work and most of the analytics, and was writing the manuscripts. In [III] the author is sharing the first authorship with Alina Lozhechnikova and was taking part in planning the work. Half of the practical work and half of the writing of the manuscript was carried out by the author. The planning of the work for the publication [IV] was performed by the author together with Dr. Julio Sánchez and most of the synthesis was carried out by the author. The manuscript was written by the author.

SUPPORTING PUBLICATIONS

1. Dax, D.; Xu, C.; Sundberg, A.; Willför, S., Synthesis of novel functional materials from *O*-acetyl galactoglucomannan using fatty acids and their properties, **2012**, Plant and Seaweed Polysaccharides Symposium, Nantes, France. (Poster Presentation)
2. Dax, D.; Xu, C.; Willför, S., Synthesis of novel functional block-copolymers from *O*-acetyl galactoglucomannan using different polymerization techniques, **2012**, 26th International Carbohydrate Symposium, Madrid, Spain. (Poster Presentation)
3. Dax, D.; Chávez, M. S.; Xu, C.; Willför, S.; Teixeira Mendonça, Sánchez, J., Cationic hemicellulose-based hydrogels for arsenic and chromium removal from aqueous solutions, **2014**, 27th ACS National Meeting, Dallas. (Oral presentation)
4. Banerjee, N. P.; Pranovich, A.; Dax, D.; Willför, S., Non-cellulosic heteropolysaccharides from sugarcane bagasse – Sequential extraction with pressurized hot water and alkaline peroxide at different temperatures. *Bioresource Technology* **2014**, 155, 446 – 450.

1. INTRODUCTION

Over the last decades, the world population was expanding rapidly from 2.5 billion in 1950 to 6.9 billion in 2010 and will reach an estimated number of almost 10 billion in 2050 (values from the United Nations). This considerable growth visualizes in a striking way which challenges humanity will face in the upcoming years, considering the problems existing already today. Everybody seeks for a comfortable, safe, and overall worth-living life. More and more people are able to raise their living standard, accompanied by an increasing need for energy, water, and raw materials. Energy is an important factor to assure the proper functionality of our society and is mostly produced by using fossil sources such coal and oil, as well as by the controlled nuclear fission. In addition to energy, also many raw materials are needed to build for example housing spaces, transportation systems and, as a relatively young development, electronic devices, for which rare and pure metals are needed. Furthermore, huge amounts of different packaging materials with tailored functionalities for everyday products are needed.

To meet up the demand of energy and raw materials, large deposits are explored all over the world. A major downside of the successful exploitation of ore mines and oil deposits is, however, the contamination of the environment, especially water, with all kinds of toxic substances. Too often, also the local population is recklessly exploited. The problems are well-known and with growing awareness of these, politics and customer behaviour started to change. There are many aspects, which have been part of discussions and decisions in the past years, just to mention the production of energy using sun and wind, implementation of recycling in the life cycle of many products, and the use of local resources in order to replace oil-based materials. The latter is a very interesting and promising development, which reveals a high potential to lead to a sustainable society in the near future, driven by the wish to keep our earth a great place to live also for the future generations. In the last decades, researchers worked on trend-setting projects, utilizing natural resources and were able to build up a strong basis for the current research efforts.

Natural resources are available all over the world in form of plants, animals, and other organisms and represent the point of origin for the design of novel, biorenewable, and biodegradable materials. Wood and wood-based materials have been used by humans since the very beginning, due to their versatility and availability in large amounts and are again gaining rising attention. Hemicelluloses and extractives from wood are now

available in a purified form and can be used for the development of novel, functional and tailored products allowing the substitution of oil-based products.

2. AIMS AND OBJECTIVES OF THIS STUDY



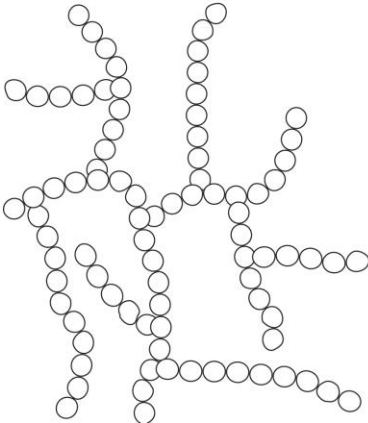

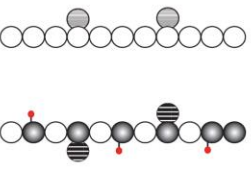
The main focus of this work, was the chemical modification of hemicelluloses from spruce wood. Firstly, the aim was to synthesize bio-based amphiphilic derivatives of *O*-acetyl galactoglucomannan (GGM) in which the hydrophilic and the hydrophobic part are composed of natural occurring materials. The idea was to apply these biomaterials to reduce the surface tension of water and to test them as additives in the paper production. Furthermore, these amphiphilic derivatives were assumed to be suitable for the modification of cellulose and nanofibrillated cellulose, and hence revealing a potential application in biocomposites. In order to generate GGM derivatives carrying polymer chains with distinguished properties, the application of controlled radical polymerization was targeted. Hereby, especially the formation of defined block-structured copolymers seemed to be of high interest. Beside the synthesis of grafted and block-structured GGM derivatives, also the production of GGM-based composites, such as films or hydrogels were kept in mind, when the work plan was elaborated.

3. BACKGROUND

Biorefinery has gained increasing attention in the last years and is affecting different areas such as agriculture and the forest industry. Since the complex technologies to convert biomass into biogas or biofuels have been optimized, more and more of the waste of the food and paper production are used in different ways to produce bioenergy. By doing so, the biopolymers present in the plant materials are degraded into smaller molecules and mixed with conventional fuels. Beside the decomposition of the biopolymers, their use as polymers has moved into the focus due to the high potential of plant-based polymeric materials to replace synthetic polymers. In wood, several polymeric materials are present, revealing distinguished properties. Cellulose is the most abundant component and represents approx. 40 % of the dry mass of wood. Lignin with 25-30 % and hemicelluloses with 20-30 % are the other main constituents of wood. Because the extraction and purification of hemicelluloses is nowadays possible to perform in an economical manner, new ways for their application have to be explored. The current work focuses on the chemical modification of water-soluble hemicelluloses extracted from softwood and some potential application areas are exploited. Before going into the experimental details, a short overview of polysaccharides and their possible chemical modification will be illustrated.

3.1 Polysaccharides

Polymers consist, according to the origin of the word polymer, of many (“polys”) parts (“meros”) (<http://www.etymonline.com/>). One group natural polymers are polysaccharides, in which the monomers consist of different monosaccharides. Polysaccharides are the main constituent of plants and have various functions ranging from structural reinforcement (mechanical properties of plant materials) over the energy storage (e.g. in seeds), to the participation in biological processes. Consequently, there are many different polysaccharides present in nature, and they have distinguished molecular build-ups, including structural features (linear or branched), weight-average molar mass (M_w) and chemical compositions (homo- or hetero-polysaccharides). Furthermore, natural polysaccharides might also contain other functional groups, such as acetyl groups or carboxylic acids.

Composition	Topology	Examples	
homopolysaccharide	linear		cellulose
	branched		galactan
	hyperbranched		starch
heteropolysaccharide	linear		glucomannan
	branched		xyloglucan O-acetyl galacto-glucomannan

○ = glucose; ● = xylose; ● = mannose; ● = galactose; ♦ = acetyl

Figure 1. Schematic illustration of selected polysaccharides, which can be found in nature and their division in homo- and heteropolysaccharides.

In Figure 1, some selected polysaccharides are schematically illustrated in order to highlight the diversity of their structures present in nature. Cellulose, most abundant polysaccharide in plants, consists of linear chains of (1→4) linked β -D-glucopyranosyl (Glc_p) units, reaching molecular weights >1000 kDa and is usually assembled in cellulose fibres and insoluble in water. As cellulose, also starch is a homopolysaccharide and only contains glucose as a monosaccharide building block. But in starch the Glc_p units are bound by α -(1→4) linkages as well as α -(1→6) linkages, and can form hyperbranched structures. Whereas cellulose has a fundamental role in the structural stability of plants,

starch represents the most common energy storage form of glucose in plants. As their function in nature, also the usability of cellulose and starch in the implementation of industrial products is different. Native cellulose is used in large amounts for the production of paper and packaging materials while starch is important for the diet of humans and animals. When modified, the use of cellulose and starch (and dextran) can be expanded to value-added products such as bioplastics and additives for the food industry.

One example of a branched homopolysaccharides is galactan, in which the main chain consists of (1→4) linked β -D-galactopyranosyl (Galp) units with a small amount of (1→6) linked β -D-galacturonic acid (GalAp) as side groups (Timell, 1982). Besides homopolysaccharides, also a large variety of heteropolysaccharides can be found in nature.

Heteropolysaccharides are featured by the presence of more than one type of monosaccharide as a building block and can either be linear or branched. One example for a linear heteropolysaccharides is glucomannan in which β -D-Glcp and β -D-mannopyranosyl (Manp) units are connected by (1→4) linkages (Sjöström, 1993). One heteropolysaccharide present in plants is xyloglucan and, as glucomannans, it is composed of two distinguished monosaccharides. But in comparison to glucomannan, the backbone of xyloglucan consists mainly of one monosaccharide ((1→4) linked β -D-Glcp and the second monosaccharide is only present as side group ((1→6) linked α -D-xylopyranosyl (Xylp)). Another, more complex heteropolysaccharide is O-acetyl galactoglucomannan (GGM), which is composed of three different monosaccharides. Because in this work GGM was used as a starting material for the synthesis of novel bio-based products, its abundance, composition and structural properties will be separately discussed in the following section.

3.2 O-acetyl galactoglucomannan (GGM)

GGM is the most abundant hemicellulose in softwood, whereby the term “hemicellulose” groups all the polysaccharides present in plant materials along with cellulose. GGM can be extracted from the wood matrix by pressurized hot-water extraction (PHWE) (Al Manasrah et al., 2012; Song et al., 2008) from Norway spruce wood (*Picea abies*). GGM consists of a linear backbone of randomly distributed (1→4)-linked β -D-Manp and (1→4)-linked β -D-Glcp units, with (1→6) linked α -D-Galp units as single side units (Capek et al., 2000; Hannuksela & Hervé du Penhoat, 2004). GGM is partially acetylated and the O-acetyl groups are located randomly at the C2 and C3

position of the mannose units in the main chain (Willför et al., 2003). In Figure 2, a segment of the GGM structure is proposed.

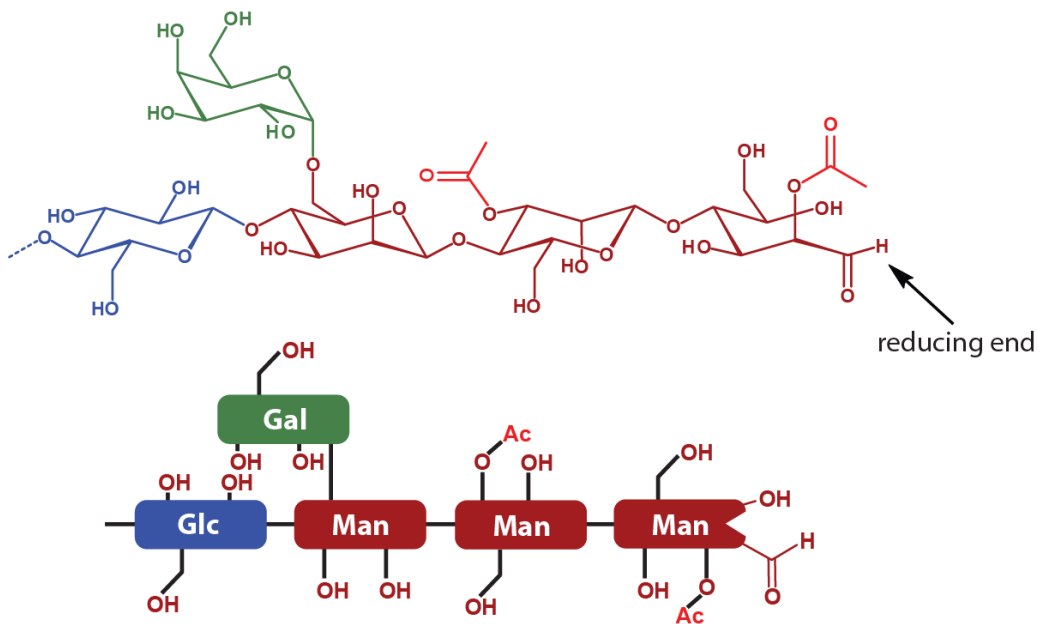


Figure 2. Chemical structure of *O*-acetyl galactoglucomannan with an open form of the reducing end sugar. Glc: β-*D*-glucopyranosyl; Man: β-*D*-mannopyranosyl; Gal: α-*D*-galactopyranosyl; Ac: acetyl group.

GGM can beside the controlled extraction from wood also be recovered from the side-streams of the pulp and paper production (Willför et al., 2003). Depending on the way of isolation and the purification method, the molar mass of GGM can vary between 5-60 kDa and the sugar ratio is approx. 3.5-4.5:1:0.5-1.1 (Man:Glc:Gal) (Willför et al., 2008). GGM shows overall a high solubility in water with a trend to be better soluble when having a low molar mass and usually results in clear, slightly brownish solutions. GGM can also be dissolved in polar organic solvents such as dimethyl sulfoxide (DMSO) and dimethylformamide (DMF), which allows the execution of well-known synthesis routes for the introduction of new functionalities to GGM. In this work esterifications, transesterifications, and reductive aminations were performed to modify GGM. Furthermore, free and controlled radical polymerization techniques were applied, resulting in novel functional GGM-based products. Some of the GGM derivatives were applied for the modification of nanofibrillated cellulose. In the following section

properties and ways of preparation of nanofibrillated cellulose will shortly be highlighted.

3.3 Nanofibrillated cellulose (NFC)

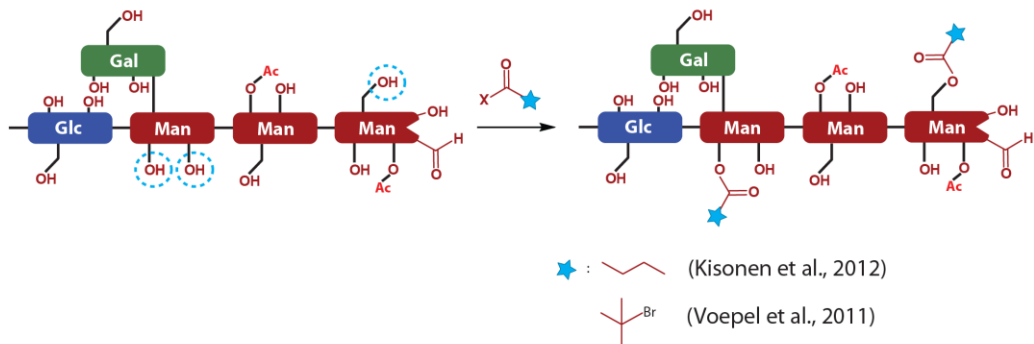
NFC represents a relatively new form of cellulose material and can be produced by bacteria (Yamanaka et al., 1989) or prepared from plant sources by mechanical disintegration of cellulose with and without pre-treatment (Missoum et al., 2013). NFC reveals an aggregate diameter ranging from 20 to 50 nm and several micrometres in length. Recent developments allow the production of NFC from wood fibers at relatively low energy consumption and the obtained NFC features a combination of high aspect ratio, high specific surface area, as well as a high strength and flexibility (Pääkkö et al., 2007). Beside an enzymatic pre-treatment (Pääkkö et al., 2007), 2,2,6,6-tetramethylpiperidine (TEMPO) mediated oxidation was proven to be an effective pre-treatment (Saito et al., 2006). NFC shows non-toxicity, biodegradability, and biocompatibility, which makes various areas of application possible (Klemm et al., 2005). So for example, NFC could be applied for the formation of aerogels (Sehaqui et al., 2011), as well as transparent films (Nakagaito & Yano, 2004). The hydrophilicity of NFC is a challenge for some applications, for example the implementation of NFC in composites (Svagan et al., 2007), and thus modifications of NFC are often necessary (Andresen & Stenius, 2007; Hubbe et al., 2008).

In the following chapters significant modifications of GGM and other polysaccharides, which have been described in literature, will be summarized.

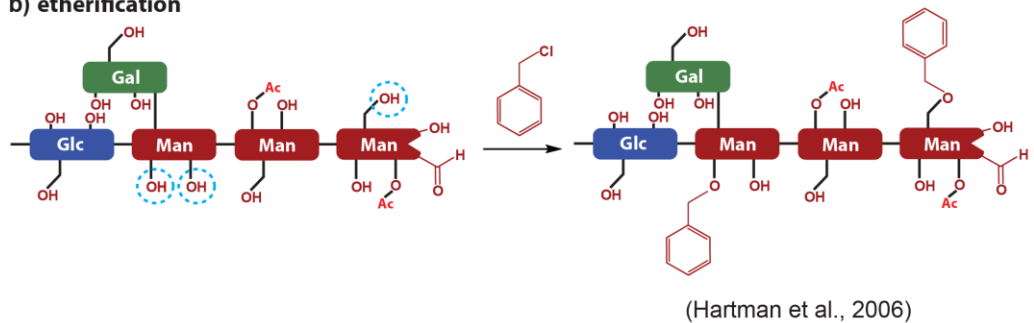
3.4 Chemical modifications of polysaccharides

Several different methods to modify GGM are known and have been described in literature. In Figure 3, a schematic overview of some reactions is presented.

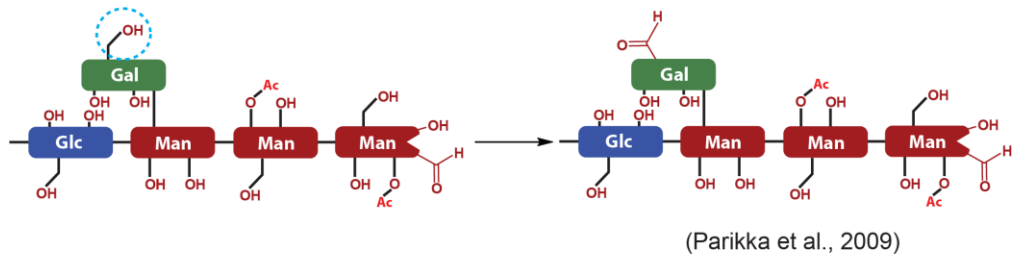
a) esterification



b) etherification



c) enzymatic oxidation



d) reductive amination

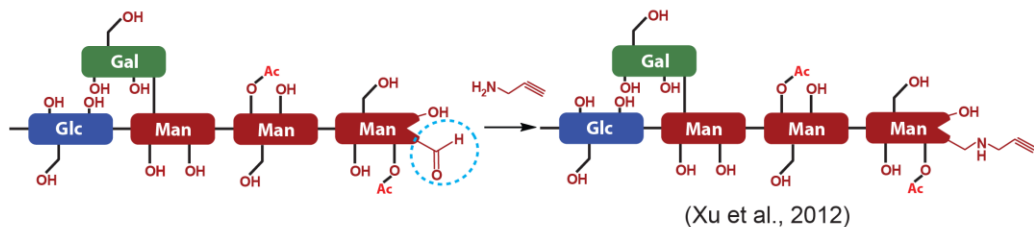


Figure 3. Examples of chemical modifications of GGM.

In the following sections the most common approaches for the chemical modification of GGM and polysaccharides in general will be given.

3.4.1 Esterification, etherification, and oxidation of polysaccharides

Two main approaches for the modification of polysaccharides are known. On the one hand the hydroxyl groups along the main chain of the polysaccharides can be modified, for example by an (trans-) esterification, etherification or oxidation. On the other hand the reducing end aldehyde group can be converted in a selective reductive amination.

The esterification is probably the most studied and utilized modification of polysaccharides due to its facility and versatility. During the esterifications, or transesterifications, the hydroxyl groups in the main chain of the polysaccharide react with, for example, an activated carboxylic acid (Enomoto-Rogers & Iwata, 2012; Voepel et al., 2011b), an anhydride (Fundador et al., 2012; Kisonen et al., 2012; Zhong et al., 2012), an ester with a good leaving group (Peng et al., 2012a), or other reactive compounds such as dimethylchlorosilanes (Goussé et al., 2004). The aim of these modifications is the introduction of new functionalities into the native polysaccharides such as hydrophobicity (Kisonen et al., 2012; Sehaqui et al., 2014), stimuli-responsiveness (Voepel et al., 2011a; Zoppe et al., 2010), ionic strength (Prado & Matulewicz, 2014) or reactive groups (azides) (Enomoto-Rogers & Iwata, 2012), as well as initiator groups (Voepel et al., 2011a) (Figure 3a). Even though most of the esterifications do not show any selective character and all the available hydroxyl groups are targeted, also selective esterifications have been reported (Heinze et al., 2006). Besides esterifications, also etherifications can be applied for the derivatization of the -OH groups in polysaccharides using e.g. benzyl chloride (Hartman et al., 2006b) (Figure 3b). Beside the mentioned reactions, polysaccharides can also react with epoxides, resulting in for example cationized products (Prado & Matulewicz, 2014).

For some applications, a selective modification of polysaccharides is necessary. For example if only a certain position in the chain should be modified, or even only a specific sugar should be targeted, catalysts like the nitroxyl radical TEMPO or enzymes such as galactose oxidase can be applied. The utilization of TEMPO was reported to selectively oxidize the carbon 6 of the sugars of polysaccharides (Davis & Flitsch, 1993; de Nooy et al., 1995) and also could be implemented for the selective oxidation of GGM (Leppänen et al., 2013). Enzymatic oxidation using galactose oxidase is even more selective than the TEMPO mediated oxidation and only specific sugar units (e.g. only galactose) can be targeted resulting in well-defined products (Parikka et al., 2009) (Figure 3c).

Apart from the hydroxyl groups along the polysaccharide chain, also the reducing end group can be triggered in controlled reactions and a few examples will be given below.

3.4.2 Reactions of the reducing end group of polysaccharides

The reductive amination of polysaccharides represents a versatile method to produce materials in which only the reducing end of the polysaccharide chain is modified, while the backbone remains in its native form. For example, for the synthesis of dextran-based surfactants, reductive amination proved to be an effective method (Bernard et al., 2008; Bosker et al., 2003; Halila et al., 2008; Hernandez et al., 2007; Schatz & Lecommandoux, 2010; Zhang & Marchant, 1994). For other polysaccharides such as xylan (Grefte et al., 2005), as well as for GGM (Xu et al., 2012) reductive amination has also successfully been used. The polysaccharide-based products formed by reductive amination have block structures, in which the native polysaccharide represents the hydrophilic block and the second block consists of a synthetic polymer or a functional group such as azides (Bernard et al., 2008) (Figure 3d). In case of surfactants the polysaccharide block is water-soluble, whereas the second block is hydrophobic (Houga et al., 2007). Besides the direct coupling of hydrophobic chains to the polysaccharide reducing end, also different controlled polymerization can be used (Schatz & Lecommandoux, 2010). Furthermore, the selective oxidation of the reducing end of cellulose for analytical purposes has been reported (Kongruang & Penner, 2004).

In the following section, the application of different polymerization techniques for design of functional polysaccharides products will be discussed.

3.4.3 Polymerization

There are many different polymers present in nature, as for example proteins which are built up by amino acids, or polysaccharides in which different monosaccharides are the building blocks. Beside these natural polymers, also synthetic polymers can be synthesized and are used in almost all the products we are using in our everyday life, reaching from packaging materials over clothing fabrics to advanced functional polymeric matrices in electronic devices. In order to obtain polymers with such different application fields, a broad range of distinguished monomers are available and have to be polymerized under specific reaction conditions. If for example the molar mass distribution of the polymer chains is not important, a free radical polymerization can be applied. In Figure 4 the simplified reaction mechanism of free radical polymerization is illustrated.

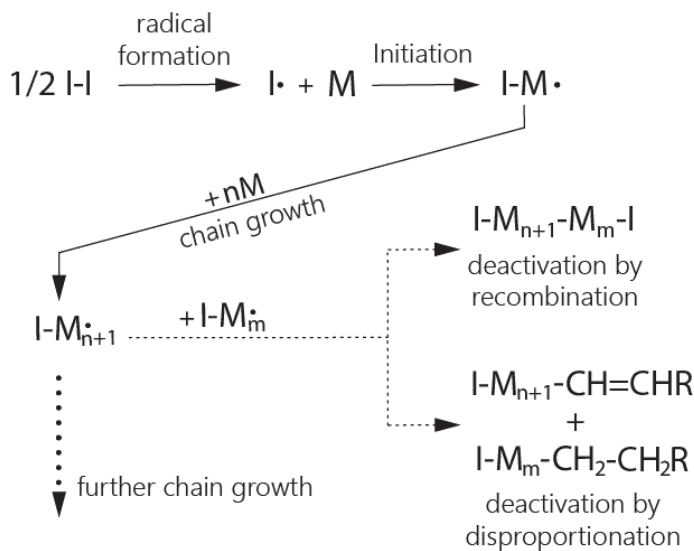


Figure 4. General schematic illustration of the reaction pathway of a free radical polymerization. I-I: initiator, M: monomer, R: monomer specific group.

In the free radical polymerization an initiator (I-I) is added to a dissolved monomer (or to the pure monomer in case of bulk polymerization) and a homolytic cleavage is induced, by e.g. heat or radiation, resulting in free radicals (I•), which can subsequently initiate the polymerization of the monomers (M). The apparent disadvantage of the free radical polymerization is that due to the high radical concentration in the reaction solution, an uncontrolled recombination of the free radicals will occur and polymer chains with different molar masses will be obtained. This is a problem when well-defined polymers are needed, having a narrow molar mass distribution, as well as an adjustable molar mass. In these cases one of the available controlled polymerization mechanisms has been used with usually higher requirements related to the reaction conditions such as oxygen-free and/or water-free reaction media.

In order to build-up block-structured, amphiphilic polysaccharide derivatives, in which the synthetic polymer chains have a defined molar mass, firstly an initiator group has to be introduced at the reducing end of the polysaccharide. Consecutively, a controlled polymerization such as atom transfer radical polymerization (ATRP) (Haddleton & Ohno, 2000; Houga et al., 2007), ring opening polymerization (ROP) (Li & Zhang, 2008), reversible addition-fragmentation chain transfer (RAFT) polymerization (Bernard et al., 2008) or single electron transfer-living radical polymerization (SET-LRP) can be performed. ATRP represents, besides RAFT, the most common method for the

controlled polymerization due to its versatility and possible application of a wide range of monomers. The controlled nature of SET-LRP, and other controlled radical polymerizations with a similar mechanism as ATRP, is given by the reversible formation of a reactive radical. Hereby the concentration of free radicals in the reaction solution is kept very low and the radicals are most of the time present in their dormant, unreactive form. This allows the suppression the unwanted recombination of active radicals and hence reduces the formation of deactivated polymer chains with uncontrolled molar masses. The reaction mechanism of SET-LRP is shown in Figure 5.

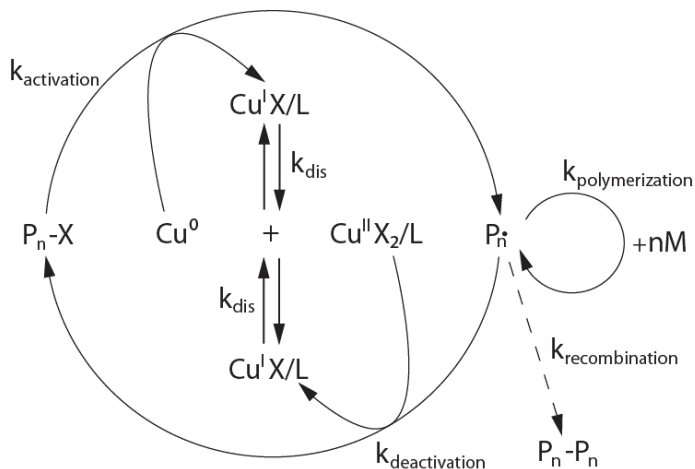


Figure 5. Mechanism of the single electron transfer-living radical polymerization (Voepel et al., 2011a).

As in ATRP, also in the SET-LRP a reversible redox process is used to control the radical concentration in the reaction solution (Percec et al., 2002). In the SET-LRP, Cu^0 is used as an electron donor, which is oxidized to Cu^I and combines with the halide atom (X), which was previously linked to the polymer chain (P_n-X). This activation step leaves an active radical at the end of the polymerization chain (active species ($P_n\bullet$)) which can react with a monomer (M), leading to the chain growth of the polymer. In the SET-LRP the concentration of this active species is very low and is rapidly transformed back into its inactive form called dormant species (P_n-X). The equilibrium of the active and the dormant species is on the side of the dormant species, assuring a low radical concentration in the reaction solution. As a consequence, the possibility of undesired recombination of two active polymer chains is drastically reduced and only minor amounts of side-products are formed. On the practical point of view, the synthesis of polymers by SET-LRP reveals some advantages compared to ATRP, because it was

proven not being sensitive to a limited amount of oxygen when organic solvents were used (Edlund & Albertsson, 2012; Fleischmann et al., 2010).

Except from the controlled polymerizations, also free radical polymerizations can be used to design functional products based on polysaccharides, such as hydrogels. A free radical polymerization distinguishes itself from ATRP or SET-LRP by the absence of a controlling agent during the polymerization, as mentioned earlier. Different initiator molecules such as azobisisobutyronitrile (AIBN) are known for polymerizations in organic solvents and ammonium persulfate for polymerizations in aqueous media. The free radical polymerization can either be used for the synthesis of linear polymer chains when only monomers with one functional group are applied or complex crosslinked networks can be designed if a crosslinking agent is added to the reaction medium. When polysaccharides are bearing two or more acrylic or methacrylic groups these can act as such a crosslinker, allowing the production of distinguished crosslinked products. Several approaches have been explored applying for example xylan, dextran or GGM as a starting material for the synthesis of hydrogels based on renewable materials (Albertsson et al., 2010; Peng et al., 2011; Prabakaran & Mano, 2006; Sá-Lima et al., 2010).

3.5 Application of chemically modified polysaccharides

Unmodified polysaccharides were used by humans since a long time ago, as for example cellulose for the production of paper. In the recent years, the interest to replace oil-based materials and the implementation of more environmentally friendly and renewable raw materials in the design of products has raised considerably. Therefore, the extracted and purified polysaccharides are modified by one of the above-described chemical or enzymatic approaches. Polysaccharides are due to their hydrophilicity suitable starting materials for the productions of block-structured surfactants. Hereby the molar masses of the polysaccharides are rather small and the amphiphilic structures have been analysed in respect to their potential self-assembly (Bütün et al., 2006; Houga et al., 2007; Li & Zhang, 2008; Liu & Zhang, 2007). The ability of some polysaccharide-based surfactants to stabilize emulsions and their potential application in cosmetic products were determined (Halila et al., 2008). Also their utilization in thermoresponsive nanoparticles (Cushen et al., 2012) and in controlled drug release systems has been studied (Suriano et al., 2010). Block-structured hemicelluloses have also been applied for the modification of cellulosic surfaces.

Unmodified and modified hemicelluloses have furthermore been applied for the production of films (Hansen & Plackett, 2008; Heikkinen et al., 2013; Kisonen et al., 2012) and barriers (Hartman et al., 2006a; Kochumalayil et al., 2013). One very promising application field for hemicelluloses are hydrogels. Hereby, modified or unmodified polysaccharides usually act as a matrix, but can also be applied as crosslinkers in the hydrogel synthesis where the resulting materials were tested for a controlled drug (Albertsson et al., 2010) and protein release (Roos et al., 2008). Furthermore, bio-based hydrogels were tested as a partially biorenewable metal ion removal material (Ayoub et al., 2013; Harihara Subramanian et al., 2008; Peng et al., 2012b). Overall, due to their high abundance in biomass, polysaccharides are one of most promising biopolymer and the current research efforts lead to the predication that polysaccharides will replace oil-based products in numerous high-value applications.

4. EXPERIMENTAL

4.1 Materials

[2-(methacryloyloxy)ethyl]trimethylammonium chloride (MeDMA) 80 wt.-% in H₂O (Aldrich), 1,1'-carbonyldiimidazole (CDI) 97 % (Aldrich), 4-(dimethylamino)pyridine (DMAP) 98 % (Aldrich), acetic acid anhydride (Riedel-de Haën, ammonium persulfate 98 % (Aldrich), bis(3-aminopropyl) terminated poly(dimethylsiloxane) (NH₂-PDMS-NH₂) (ABCR), copper bars (99.999 %) (Aldrich), Di-*tert*-butyl-dicarbonate (BOC₂O) (Aldrich), ethylenediamine (EDA) ≥99.5 % (Aldrich), Glycidyl methacrylate (GMA) 97 % (Aldrich), HNO₃ (Merck), K₂Cr₂O₇ (Merck), Methyl methacrylate (MMA) 99 % (Aldrich), myristic acid 99.5 % (Fulka), Na₂HAsO₄•7H₂O (Merck), NaOH (Merck), N-isopropylacrylamide (NIPAM) (Aldrich), pelargonic acid ≥97 % (Fulka), sodium cyanoborohydride 95% (Aldrich), stearic acid 99 % (Merck), triethylamine (Et₃N) 99 % (Aldrich), trifluoroacetic acid (TFA) 99 % (Aldrich), tris(2-aminoethyl)amine 96 % (Aldrich), α-bromoisobutyl bromide (BIBB) (Aldrich), dimethyl sulfoxide (DMSO) (Merck), methyl *tert*-butyl ether (MTBE) (Fulka), dimethylformamide (DMF) (Aldrich), acetone (J.T. Baker), ethanol (EtOH) (Merck). All chemicals were used as received when not mentioned differently.

Two different GGM fractions have been used in this work. For the publications [I-III] a GGM with a M_w of 7.1 kDa with a polydispersity index (PDI) of ~1.5 was used. This fraction was extracted from Norway spruce (*Picea abies*) wood applying the conditions studied in a previous work (Kilpeläinen et al., 2013; Song et al., 2008). A concentrated hot-water extract (30 wt.-%) was provided by The Finnish Forest Research Institute – Metla. The extract was further purified in order to remove lignin residues and to narrow down the molar mass distribution (low PDI). Therefore, the concentrated GGM solution (330 mL) was diluted with water (670 mL) and then precipitated in 9 L of ethanol at room temperature. The white precipitate was filtrated off and consecutively washed with ethanol, acetone, and methyl *tert*-butyl ether. For the publication [IV] another GGM fraction with a M_w of 28 kDa and a PDI of ~1.3 was applied. This GGM was isolated from the process water of thermomechanical pulping (TMP) using spruce prior to any chemical treatments (Willför et al., 2003). In short, the process water was purified from colloidal wood resin, and aromatic residues using a cationic coagulant (Raifix 120, Raisio Chemicals Oy, Finland) and XAD-7 resin (Amberlite, Rohm and Haas, UK). The solution was then concentrated under reduced pressure before GGM was collected by precipitation in ethanol. The sugar ratio of GGM was determined by acid methanolysis and was around 5-4:1:0.5-1.1 (Man:Glc:Gal) and the degree of acetylation (DS_{Ac}) ~ 0.20

(Willför et al., 2008). The GGM fraction with a number-average molar mass (M_n) of 4.7 kDa was referred as *GGM* [I-III] or *GGM5* [IV]. The GGM fraction with a number-average molar mass of 21.5 kDa was labelled as *GGM22* [IV].

4.2 Methods

4.2.1 High Performance Size Exclusion Chromatography (HPSEC) [I-IV]

M_w and M_n (and the PDI) of native GGM were determined by high performance size exclusion chromatography (HPSEC) in on-line combination with a multi-angle laser light scattering (MALLS) instrument (miniDAWN, Wyatt Technology, Santa Barbara, USA) and a refractive index (RI) detector (Shimadzu Corporation, Japan). A two-column system, 2 × Ultrahydrogel™ linear 300 mm × 7.8 mm column (Waters, Milford, USA), in series was used. 0.1 M NaNO₃ was used as the elution solvent. The flow rate was 0.5 mL/min. A dn/dc value of 0.150 mL/g was used (Michielsen et al., 1999). The samples were filtered through a 0.22 µm nylon syringe filter before injection. The injection volume was 100 µL. Astra software (Wyatt Technology, Santa Barbara, USA) was used to analyse the data.

Some of the prepared GGM derivatives showed low water solubility and in order to avoid the formation of aggregates during the HPSEC measurement, the samples were acetylated and tetrahydrofuran (THF) was used as a solvent. Therefore, 2 mg of material were treated with 250 µL of pyridine and 250 µL of acetic acid anhydride at 70 °C for 2 h. The excess of acetic acid anhydride was neutralized with methanol and the volatile compounds were removed in N₂ flow. The derivatized samples were dissolved in 2 mL of THF and filtered through 0.45 µm PTFE syringe filter. M_w and M_n of the acetylated products were determined by HPSEC using polystyrene standards for calibration after recording retention volumes with a SEDEX Model 85 ELSD detector (SEDERE, Alfortville France). A two-column system, 2 × JordiGel DVB 500Å 300 mm x 7.8 mm (Jordi Labs, Mansfield, MA, USA), in series was used. THF containing 1 % (v/v) acetic acid was used as eluent and the flow rate was 0.8 mL/min. The data was analysed with Shimadzu software packages CLASS VP 6.1 and GPC for CLASS VP (Shimadzu Corporation, Japan).

4.2.2 Nuclear Magnetic Resonance spectroscopy (NMR) [I-IV]

The native GGM and its derivatives were analysed by ¹H and ¹³C NMR measurements using a Bruker Avance spectrometer (operation frequency: ¹H: 600.13 MHz; ¹³C: 150.92 MHz). For the water-soluble products, D₂O was used as a solvent and the water insoluble products were dissolved in DMSO-*d*₆. For the ¹³C measurements in water, DMSO-*d*₆ was

used as an internal standard. For the nonpolar components, CDCl_3 was used as a solvent. To assure a good resolution, the temperature was varied between 25 and 35 °C depending on the sample.

4.2.3 Calibration of the ^1H NMR spectra

For quantitative evaluation of the proton spectrum, the theoretical integration value for the peak region from 3.2 to 4.4 ppm was determined. Beforehand, size exclusion chromatography for native GGM and a volumetric titration for the determination of the acetyl-group content were performed. For the calculations, the average molar mass ($M_n = 4.7 \times 10^3$ g/mol) was used. The volumetric titration gave a value of 1.16 mmol/g (acetyl group per gram of GGM). The amount of acetyl groups per GGM chain was calculated as shown in equation (1),

$$n_a = M_n \times 1.16/1000 = 4700 \times 1.16/1000 = 5.5 \quad (1)$$

where M_n is the number-average molar mass of GGM and n_a is number of acetyl-groups per GGM chain (degree of acetylation).

The degree of acetylation of GGM was 5.5 (referred to one GGM chain). The amount of sugar units in a GGM chain with a molecular weight of 4.7×10^3 g/mol containing 5.5 acetyl groups per macromolecule was determined using equation (2), knowing that the average molecular weight of each anhydro-monomer unit was $M_s=162$ g/mol,

$$n_s = (M_n - n_a \times M_a)/M_s = (4700 - 5.5 \times 43)/162 = 28 \quad (2)$$

where M_n is the number-average molar mass of GGM, n_a is the number of acetyl-groups per GGM chain, M_a is the molar mass of one acetyl-group, and M_s is the average molar mass of one sugar unit in GGM.

The total mass of the 5.5 acetyl groups was subtracted from M_n , and it was found that, on average, one GGM chain consisted of 28 sugar units. For the determination of the theoretical value for the integration of the area between 3.2 and 4.4 ppm in the proton NMR spectra, the amount of protons showing a signal in this area had to be determined. Every sugar unit has 7 protons, which can be detected by proton NMR. With 28 sugar units per chain, there were a total of 196 protons for each GGM chain. There are two distinguished regions in the proton spectrum of GGM, the first from 3.2 to 4.4 ppm and the other from 4.6 to 5.5 ppm. The region between 4.6 and 5.5 ppm contains signals of the reducing end protons as well as the protons in the neighbourhood of the acetyl

groups, resulting in $28+5.5=33.5$ protons. Subtracting 33.5 protons from the total number of protons gave 162.5 protons, which was taken as the theoretical value for the integration of the peak region from 3.2 to 4.4 ppm. This value was set as a constant for all the spectra evaluated in this work, and the products were determined to be solvent-free before measuring the ^1H NMR spectra.

4.2.4 Fourier Transformed Infrared Spectroscopy (FTIR) [I-IV]

The infrared spectroscopy measurements were performed with a Bruker ALPHA series using the ALPHA platinum ATR single reflection diamond ATR module. The samples were directly placed on the ATR plate for the measurement. The results were evaluated using the software OPUS from Bruker.

4.2.5 Thermal Gravimetric Analysis (TGA) [I, II]

The thermal stability of GGM and GGM-fatty acid derivatives was investigated by DSC-TGA (Differential Scanning Calorimetry-Thermal Gravimetric Analysis) (Q600, Ta Instruments). The samples were dried before thermal analysis. The heating rate in the experiments was $10\text{ }^\circ\text{C}/\text{min}$ up to $600\text{ }^\circ\text{C}$ under nitrogen. A platinum cup was used in these tests. The weight of the sample and the DTA-signals (the difference between the sample and reference temperature) were recorded.

4.2.6 Quartz Crystal Microbalance with Dissipation Monitoring (QCM-D) [III]

The in-situ adsorption of GGM and its derivatives on ultrathin NFC films was monitored using a QCM-D instrument (E4, Q-Sense AB, Västra Frölunda, Sweden). The technique is based on the changes in oscillation of a quartz crystal caused by changes in mass. With E4 instrument, changes in frequency and dissipation energy (frictional losses due to viscoelastic properties of the adsorbed layer, ΔD) can be monitored simultaneously. During adsorption the oscillation frequency of the crystal increases and deviation from the fundamental frequency (5 MHz) and its overtones (15, 25, 35, 55, and 75 MHz) is detected. According to the Sauerbrey equation (3) (Sauerbrey, 1959), the change in frequency (Δf) is proportional to the mass adsorbed per unit surface (Δm),

$$\Delta m = (-C\Delta f)/n \quad (3)$$

where C is the sensitivity constant (here $C=0.177\text{ mg}/\text{m}^2$) and n is the overtone number (here $n=3$). The equation 1 is valid for thin, rigid, and uniform films, but it underestimates mass for viscoelastic films, when $\Delta D > 1$ (Höök et al., 2001). Therefore, the calculated mass values presented in this work are estimations and should not be used as absolute values. GGM and the GGM derivatives were dissolved in pure water to

0.5 g/L concentration. The flow rate through the QCM-D chambers was set to 0.1 mL/min and kept constantly during the measurements.

4.2.7 Oxygen Transmission Rate (OTR) [III]

The measurements were performed with Oxygen Permeation Analyser Models 8001 and 8011 (Systech Instruments Ltd, UK) with two replicates. The tests were carried out at 23 °C temperature and 0 % and 80 % relative humidity using metal masks with a test area of 5 cm². The coated side of the samples faced the test gas (100 % oxygen). OP was calculated by multiplying OTR value by the thickness of the sample. The presented values are average of two measurements.

4.2.8 Water Contact Angle (CA) [III]

CA of water on pure and coated NFC films were determined using the CAM 200 (KSV Instruments Ltd., Helsinki, Finland) contact angle meter with computer based controlling system and capturing video camera. The static sessile drop method was employed in the measurements and CA was determined for at least three spots on each sample. The tests were performed with pure water at room temperature, and droplet volume of 6.7 µL was used. The full Young-Laplace equation was used to determine the contact angle shape of the sessile drop.

4.2.9 Determination of the surface tension in water [I, III]

The surface tension of the GGM and its derivative solutions was measured by the Du Noüy ring method using a KSV Sigma 70 Tensiometer. The used Pt-Ir ring was rinsed with ethanol with consecutive drying after each measurement to ensure zero contact angle. The real tension values were immediately determined for different concentrations of the surfactants at 25 °C. The equilibrium time for all the samples was set to 5 min. The surface tensions were plotted versus the logarithm of the surfactant concentration (mg/mL) and the respective critical aggregation concentrations (CAC) or critical micelle concentration (CMC) was determined graphically from the drastic change of the slope (Jönsson et al., 1998).

4.2.10 Determination of the Area (A) occupied by the adsorbed molecules at the water-air interface

The surface excess, Γ (mol/m²), was calculated using the Gibbs adsorption isotherm,

$$\Gamma = -(1/RT) \times (d\gamma/d\ln C) \quad (4)$$

where R is the ideal gas constant (8.314 J/(mol*K)), T is the absolute temperature during the measurement (Jönsson et al., 1998), while $d\gamma/d\ln C$ was estimated from the plots of the respective surface tension versus the natural logarithm of the concentration of the surfactant when the concentration approaches the CAC. In the cases where the CAC could not be determined because of precipitation of the sample at high concentration, the slope was estimated using the data points available. The cross sectional area per surfactant molecule, A (\AA^2), was subsequently calculated from,

$$A = 1/(N_A\Gamma) \quad (5)$$

where N_A is the Avogadro's number. The water used for the surfactant solutions was purified by a Millipore system and had surface tension of ~ 73 mN/m.

4.2.11 Swelling of the GGM-based hydrogels [IV]

The swelling ratio was determined by placing 100-200 mg of the dried GGM-based hydrogel in 200 mL of de-ionized water. After 24 h at room temperature, the hydrogel was removed from the solution. Water that remained on the surface of the hydrogel was carefully removed using a paper filter. The weight of the swollen hydrogels was determined and the swelling ratio (Q) was calculated using equation (6).

$$Q = (m_t - m_o)/m_o \quad (6)$$

where m_t is the weight of the hydrogel at the time t and m_o is the initial weight of the oven dried sample (Albertsson et al., 2010; Zheng et al., 2013).

4.3 Synthesis

In this work, distinguished modifications of GGM were performed in which either the hydroxyl groups in the GGM chain were converted or the reducing end was targeted in a selective reaction. Furthermore, several other intermediate products were prepared and characterized before converting with GGM.

4.3.1 Synthesis of Me₆-TREN [II]

Me₆-TREN was synthesized as reported earlier (Ciampolini & Nardi, 1966). Formic acid (15.7 g of 98 % (v/v) solution, 0.34 mol, 10 eq.) and formaldehyde (6.8 g of 37 % (v/v) solution, 0.23 mol, 6.7 eq.) were mixed in a round-bottled flask and cooled down to 0 °C using an ice bath. Consecutively tris(2-aminoethyl)amine (5 g, 0.034 mol, 1 eq.) in 20 mL of H₂O was added dropwise to the mixture and the temperature was kept below 4 °C. After the addition of the tris(2-aminoethyl)amine, the reaction mixture was stirred

for 1 h at 0 °C and then slowly heated up to 100 °C. The reaction was kept at 100 °C for 15 h and then the volatile compounds were evaporated under reduced pressure. The pH of the orange residue was adjusted to 10 using a 1 M NaOH solution. The crude product was collected by extracting with dichloromethane and consecutively washed with a saturated NaCl solution and H₂O. After evaporation of the organic solvent, the product was obtained as clear yellow oil (1.4 g, 8.9 mmol, 26 % yield).

4.3.2 Preparation of *tert*-butyl-*N*-(2-aminoethyl) carbonate (NH₂-BOC) [I, II]

The synthesis of the amino functional coupling agent containing the initiator group has been synthesized previously (Houga et al., 2007) and a similar synthesis route was applied. A solution of di-*tert*-butyl-dicarbonate (BOC₂O) (17.5 g, 80 mmol) in 180 mL of 1,4-dioxane was dropped into a stirred solution of ethylenediamine (36 g, 600 mmol, 7.5 eq.) in 180 mL of 1,4-dioxane over a period of 5 h at room temperature. After additional 48 h stirring at room temperature, the formed precipitate was filtered off and the solvent was evaporated at reduced pressure. To the residue, 300 mL distilled water was added and the water-insoluble bis(*N,N'*-*tert*-butyloxycarbonyl)-1,2-diaminoethane was removed by filtration (Sadhu et al., 2004). The product was extracted by dichloromethane from the aqueous solution saturated with NaCl. The organic phase was dried over Na₂SO₄ and the solvent was evaporated under reduced pressure to give *tert*-butyl-*N*-(2-aminoethyl) carbonate (NH₂-BOC) (7.68 g, 48 mmol, 60 % yield).

4.3.3 Amidation of α -bromoisobutyryl bromide (BIBB) with NH₂-BOC [III]

BIBB (16.6 g, 72 mmol, 1.5 eq.) in 50 mL of THF was slowly added to a solution of NH₂-BOC (7.68 g, 48 mmol, 1 eq.) in THF (150 mL) in the presence of Et₃N (9.7 g, 96 mmol, 2 eq.). The temperature during the addition of BIBB was kept at 0 °C. After 1 h the addition was completed and the solution was stirred for 24 h at room temperature. The formed triethylammonium bromide was filtered off as a white solid. The organic solvent was removed under reduced pressure and the crude product was redissolved in methanol and precipitated into water saturated with Na₂CO₃. After drying the product was collected as a white solid (11.0 g, 35.6 mmol). The BOC-protected initiator (11.0 g, 35.6 mmol, 1 eq.) was dissolved in 70 mL of ethyl acetate and hydrogen chloride gas was bubbled into the solution (Cushen et al., 2012). An excess of hydrogen chloride gas was formed by the addition of a 37 % hydrogen chloride solution into concentrated H₂SO₄. After the bubbling was completed the reaction mixture was stirred for 1 h at room temperature. The organic solvent was evaporated under reduced pressure. To the residue, 40 mL of water was added and the insoluble fraction was filtered off. The

aqueous fraction was freeze-dried and yielded a white solid (NH₂-Br) (7.2 g, 34.5 mmol, 72 % yield).

4.3.4 Synthesis of the GGM macroinitiator [II]

GGM (2.38 g, 0.50 mmol, 1 eq.) was dissolved in 90 mL H₂O and NH₂-Br (0.63 g, 3 mmol, 6 eq.) was added. The solution was heated up to 50 °C and the pH was adjusted to 4. Consecutively, NaBH₃CN (1.5 g, 23.9 mmol, 50 eq.) was added to the solution and the reaction mixture was stirred at 50 °C. After 8 h NaBH₃CN (1.5 g, 23.9 mmol, 50 eq.) was added and the reaction was stirred for another 16 h at 50 °C. The reaction was stopped and the reaction solution was precipitated in 800 mL of cold EtOH with a subsequent filtration of the product. The solid product was re-dissolved in H₂O and dialyzed against distilled H₂O. After freeze-drying, a white solid was obtained (1.1 g, 0.23 mmol, 46 % yield). The product was analysed by ¹H and ¹³C NMR and the results are presented in the result and discussion section.

4.3.5 SET-LRP using the GGM macroinitiator [II]

For the polymerizations, three different unsaturated monomers (MeDMA, NIPAM, and MMA) were used. Before starting the polymerizations, DMSO, H₂O and MMA were distilled and kept under argon. A solution of Me₆-TREN (0.05 mol/L) in DMSO was prepared and kept under argon. The polymerizations using the different monomers were conducted under similar conditions; in the following the procedure is exemplary shown for NIPAM. GGM-Br (49.4 mg, 0.01 mmol, 1 eq.), 5 pieces of copper and NIPAM (50 mg, 0.44 mmol, 44 eq.) were introduced in a Schlenk tube equipped with a magnetic stirrer. The tube was consecutively degassed under argon (3 cycles) and 3 mL of H₂O and 1 mL of DMSO were added. The reactants were dissolved by stirring at 40 °C and the solution was again degassed carefully under argon (3 cycles). To start the polymerization, the Schlenk tube was transferred to an oil bath (40 °C) and then Me₆-Tren (100 µL of the previous prepared solution, 1.15 mg, 0.005 mmol, 0.5 eq.) was added. After 30 h the copper pieces were removed and the reaction mixture was precipitated in cold acetone. The product was collected by centrifugation and washed twice with cold acetone. To remove copper residues, the product was dissolved in distilled water and dialyzed against distilled water. The purified copolymer was received after freeze-drying. For the polymerization of MeDMA the same solvent mixture was applied as for NIPAM, but for MMA, pure DMSO (4 mL) was used. The GGM-block-pMMA derivatives were not soluble in water and in order to remove solvent and copper residues the samples were swollen in water and transferred to dialyses tubes with consecutive dialyses against distilled water.

4.3.6 Activation of the fatty acids [I]

Three fatty acids (pelargonic acid: C9; myristic acid: C14; stearic acid: C18) were equally modified and the reaction procedure is exemplarily described for stearic acid. Stearic acid (5.0 g, 17.58 mmol) was dissolved in 50 mL of THF and CDI (3.4 g, 21.1 mmol, 1.2 eq.) was added. The reaction mixture was stirred at room temperature and the progression of the reaction was followed by observing the emission of CO₂ with a gas bubbler. After the CO₂ formation ended, the reaction was stirred at room temperature for one additional hour. Subsequently, 100 mL of distilled water was added and the precipitated product was filtered off followed by freeze-drying from water to yield the imidazole derivative of stearic acid as a colourless powder (5.2 g, 15.6 mmol, 88 % yield).

4.3.7 Amidation of the activated fatty acids with NH₂-BOC [I]

The activated stearic acid (1 g, 3 mmol) was dissolved in 25 mL THF at 45 °C under stirring. NH₂-BOC (0.86 g, 5.4 mmol, 1.8 eq.) was added to the reaction flask and to catalyse the reaction, Imidazole (0.41 g, 6 mmol, 2 eq.) was added. The reaction mixture was kept at 45 °C under stirring overnight and then 60 mL of distilled water was added. The precipitated product was filtered off and freeze-dried. The dried product was dissolved in 25 mL dichloromethane and CF₃COOH (5 mL, 29 mmol, 10 eq.) were added. The reaction was stirred for 3 h at 40 °C and subsequently the solvent and the excess of CF₃COOH were evaporated under reduced pressure. The residue was dissolved in dichloromethane and washed with a 0.5 molar NaOH solution and with distilled water saturated with NaCl consecutively. The organic phase was dried over Na₂SO₄ and the solvent was removed in vacuum. The product (C18-NH₂) was obtained as a colourless solid (0.55 g, 2.8 mmol, 56 % yield).

4.3.8 Esterification of GGM with activated fatty acids [I]

GGM (1 g, 0.2 mmol) was added to 15 mL of a mixture of DMSO and THF (ratio 2:1) and heated up to 50 °C. Under stirring activated stearic acid (134 mg, 0.4 mmol, 2 eq.) and imidazole (54 mg, 0.8 mmol, 4 eq.) were added. The reaction mixture was stirred at 50 °C for 15 h and then precipitated in ethanol. The precipitate was filtered off and washed with ethanol and acetone consecutively. After drying in the vacuum oven at 40 °C the crude product was re-dissolved in distilled water and dialyzed against distilled water for 48 h to remove solvent residues. Not all the products were soluble in water and a water-soluble and a water insoluble fraction were separated. After removing the water by freeze-drying the product fractions were obtained as brownish solid (detailed yields and compositions are listed in Table 1).

4.3.9 Reductive amination of GGM using amino functional fatty acids [I]

GGM (1 g, 0.2 mmol) was dissolved in 50 mL of a mixture of DMSO and ethanol (ratio 3:2). C18-NH₂ (327.5 mg, 1.0 mmol, 5 equiv) was added into the reaction flask and the mixture was heated up to 50 °C. After stirring for 30 min a homogenous solution was obtained and NaBH₃CN (628 mg, 10 mmol, 50 equiv) was added. After 48 h stirring at 50 °C, a second portion of NaBH₃CN (628 mg, 10 mmol, 50 equiv) was added and the reaction was stirred for another 24 h and then stopped. The reaction mixture was precipitated in ethanol and recovered by centrifugation. The precipitate was washed with ethanol and acetone consecutively and then dried in the vacuum oven for 48 h at 40 °C. To remove DMSO residues the product was re-dissolved in distilled water and dialyzed against distilled water. After the dialysis, the water was removed by freeze-drying and the product was obtained as a light brownish solid (420 mg, 0.078 mmol, yield 40 %).

4.3.10 Synthesis of GGM-block-PDMS [III]

For the reductive amination of GGM with NH₂-PDMS-NH₂, a 20-fold excess of the NH₂-PDMS-NH₂ was used to assure the formation of AB-block structured derivatives and to avoid the formation of ABA-block structured derivatives. GGM (5 g, 1.05 mmol, 1 eq) was dissolved in 125 mL of DMSO and the temperature was adjusted to 50 °C. A solution of NH₂-PDMS-NH₂ (18.95 g, 21.05 mmol, 20 eq.) in 50 mL of THF was prepared and the amine groups were protonated using aqueous H₂SO₄. Consecutively, the NH₂-PDMS-NH₂ solution was quickly added to the GGM and the pH was verified to be around 4. After stirring for 1 h at 50 °C, NaBH₃CN (3.31 g, 52.7 mmol, 50 eq.) was introduced to the homogenous reaction mixture and the stirring was continued at a high speed for 24 h. Then a second addition of NaBH₃CN (3.31 g, 52.7 mmol, 50 eq.) was performed in order to ensure complete conversion of all the GGM reducing ends. After 24 h additional stirring at 50 °C the reaction mixture was precipitated in 700 mL of EtOH. The product was filtered off and redissolved in distilled water and precipitated for a second time in EtOH in order to remove unreacted residues of NH₂-PDMS-NH₂. Consecutively, the product was dissolved in a small amount of distilled water and dialyzed (cut-off 2 kDa) against distilled water for 48 h while the water was renewed every 12 h. Finally, the solution was freeze-dried to result in a white solid (3.17 g, 0.55 mmol, 56% yield).

4.3.11 Synthesis of GGM-MA macromonomers [IV]

The reaction conditions for the insertion of the methacrylate groups into the GGM chain were adjusted outgoing from a previous study (Peng et al., 2012a) by changing the temperature, the catalyst amounts, and the solvent. The parameters of the performed reactions are listed in Table 3. The exact procedure is exemplarily described for the

product GGM5-MA0.03 (here 0.03 denotes the degree of substitution of GGM5). GGM5 (100 mg, 0.62 mmol of anhydrous sugar units, 1 equiv.) was dissolved in 3 mL of dry DMF at 50 °C. Consecutively DMAP (5 mg, 0.041 mmol, 5 wt.-% in respect to GGM) and GMA (62 mg, 0.43 mmol, 0.70 equiv.) were added and the mixture was stirred under nitrogen atmosphere at 50 °C for 16 h. The reaction mixture was then transferred into a dialyses tube (cut-off of 2 kDa) and dialyzed against distilled water for 3 days with daily water exchange. The aqueous solution of the product was dried by consecutive evaporation under reduced pressure and storage in the oven at 50 °C overnight. A brownish solid was obtained (62.7 mg, yield 62 %).

4.3.12 Synthesis of the GGM-based hydrogels [IV]

Exemplary the synthesis of [GGM5-MA0.14;20;10;5] is described. The products of the polymerization were labelled as follows: [(GGM-MA derivative used); (wt.-% of GGM-MA + monomer in the reaction solution); (wt.-% of GGM-MA in respect to the monomer); (mol-% of the initiator in respect to the monomer)]. GGM5-MA0.14 (50.0 mg, 0.01 mmol), MeDMA (450 mg, 2.16 mmol) and ammonium persulfate (24.7 mg, 0.11 mmol) were dissolved in 2.5 mL of de-ionized water and N₂-gas was bubbled into the solution for 15 min in order to remove oxygen. Subsequently the reaction tube was placed in an oil bath at 75 °C for 2 h. After the reaction was completed, the formed hydrogel was placed in 200 mL of de-ionized water in order to remove unreacted monomers and loose polymer chains from the hydrogel. After drying in the oven at 40 °C, a pure GGM-based hydrogel was obtained.

5. RESULTS AND DISCUSSION

5.1 Overview of the experiments

In this work different chemical modifications of GGM were performed by substituting the hydroxyl groups of the main chain or the reducing end aldehyde group. In a first approach, GGM was derivatized with three different fatty acids resulting in amphiphilic copolymers in which the hydrophilic part (GGM) and the hydrophobic part (fatty acids) were of natural origin. The produced amphiphilic molecules had either grafted or defined block structure (Figure 6a) [I]. The GGM block-structured derivatives were tested with respect to their potential to be applied for the modification of cellulosic surfaces using QCM-D [III]. In a second reaction set, a GGM macroinitiator was established in which an initiator group for polymerization was introduced to the reducing end of GGM [II]. This GGM macroinitiator was consecutively applied for the synthesis of well-defined GGM-*block*-copolymers using three distinguished monomers in a controlled polymerization (Figure 6b). In a third approach, GGM macromonomers were synthesized by transesterification and further applied in the production of cationic hydrogels with tailored physical properties using a cationic monomer (Figure 6c) [IV]. The distinguished GGM derivatives were completely characterized by means of their chemical composition and tested with respect to their potential application in different areas.

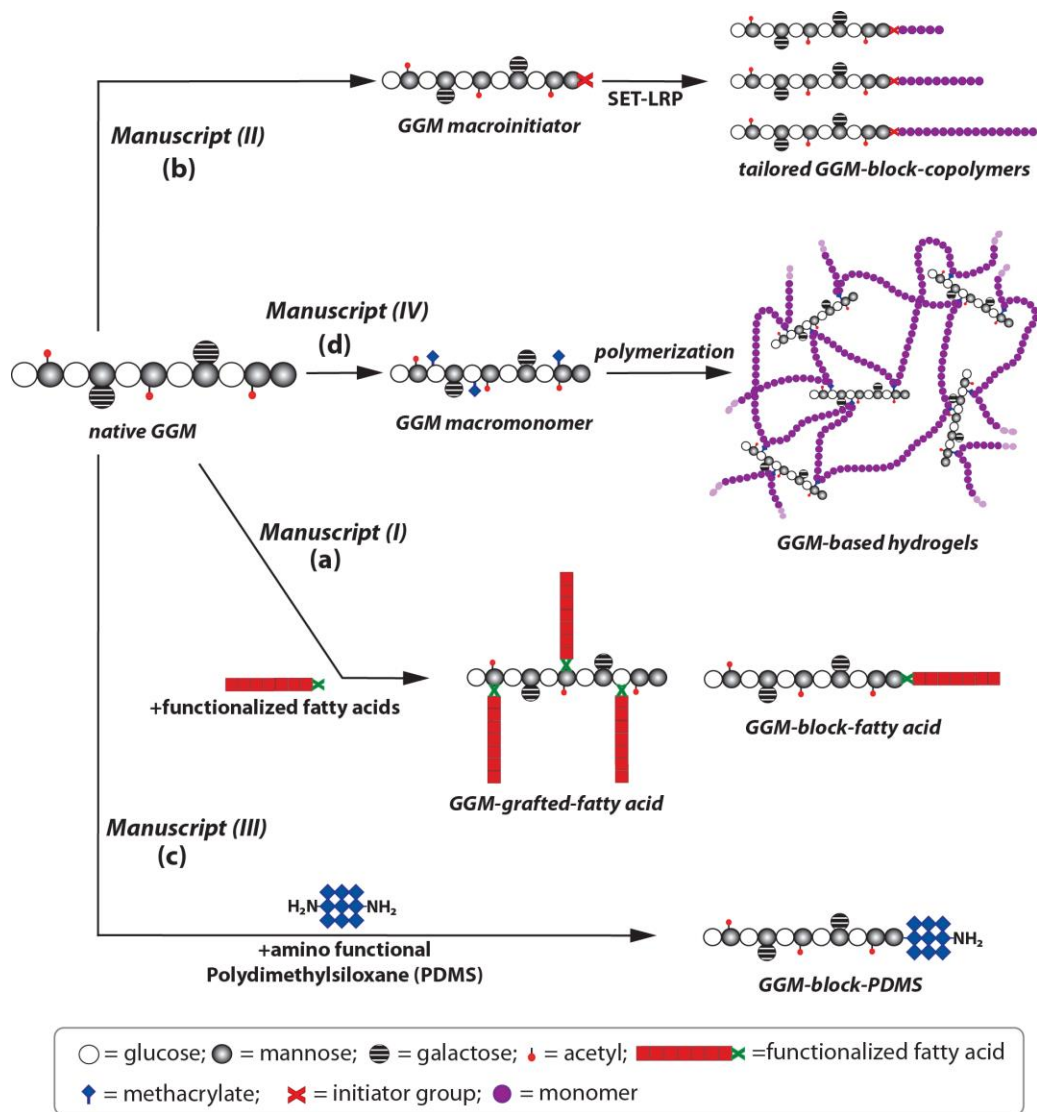


Figure 6. Overview of the performed derivatizations of GGM and their chemical structures. (a) Grafted and block structured GGM-fatty acid derivatives (Section 5.2.1) and their application (Section 5.3.1 and 5.3.2); (b) functional GGM-block structured derivatives by polymerization (Section 5.2.3); (c) Synthesis of a GGM-block-PDMS (Section 5.2.2) and its application (Section 5.3.2); (d) GGM-based hydrogels (Section 5.2.4) for purification of aqueous solutions (Section 5.3.3).

5.2 Synthesis of GGM derivatives

5.2.1 Amphiphilic GGM-fatty acid derivatives [I]

The aim of this part of the work was the synthesis of novel amphiphilic GGM derivatives using naturally-occurring fatty acids as a hydrophobic component [I]. Fatty acids derivatized polysaccharides have been described earlier and so for example grafted cellulose and starch were obtained by esterification (Grote & Heinze, 2005; Hussain et al., 2004; Vaca-Garcia et al., 1998). Hereby relatively high temperatures were applied and the resulting cellulose derivative had a high DS values. Beside the application of acid halides, also CDI was reported as a suitable activating agent for carboxylic acids, allowing less harsh reaction conditions. Because the application of low temperatures is desirable when working with GGM, in order to avoid degradation, three different fatty acids (pelargonic acid: C9; myristic acid: C14; stearic acid: C18) were applied and were in a first step activated using CDI. The activated fatty acids were then converted in an esterification reaction with GGM to result in GGM-grafted-fatty acids (B in Figure 7) or used as a starting reagent for the synthesis of amino functional fatty acid derivatives (A in Figure 7).

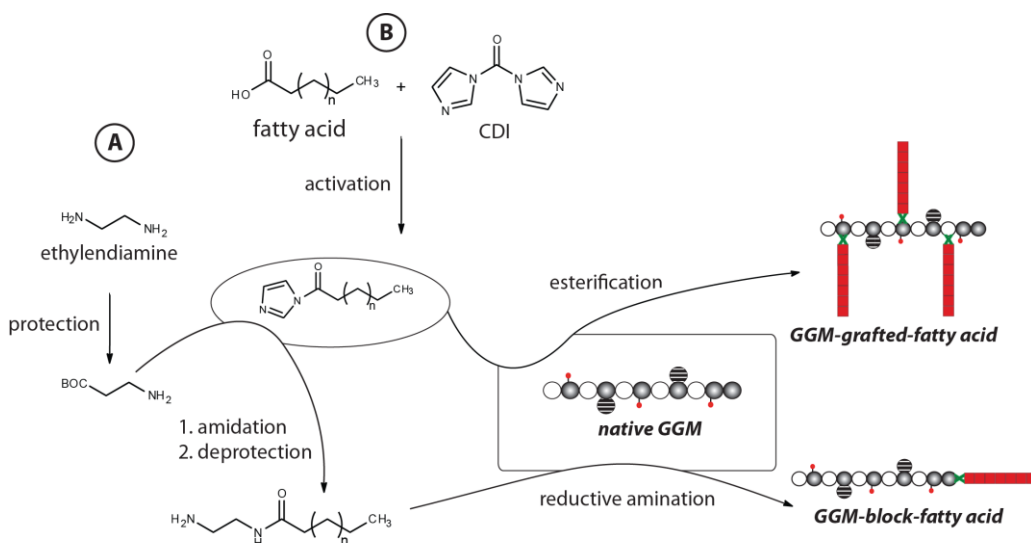


Figure 7. Reaction pathway for the formation of GGM block- (A) and grafted-fatty acid (B) derivatives.

A widely used and comparably cheap method for the activation of carboxylic acids is based on the application of thionyl chloride, resulting in highly reactive acid chlorides.

These acid chlorides can be implemented in esterification reactions with high conversion of the corresponding alcohols while releasing HCl as a side product. When GGM would be used as a polyalcohol, the formation of HCl and the hence drop of the pH value in the reaction solution could lead to partial degradation of the GGM molecules. To avoid an unwanted degradation of GGM during the esterification, the fatty acids were activated by CDI. CDI exhibits several advantages compared to thionyl chloride such as its convenience in handling and lack of HCl formation during the esterification together with a high reactivity. The three fatty acids were activated this way and were recovered after the activation reaction in high yields and in pure form as confirmed by ^1H NMR. For the esterification of GGM using the activated fatty acids, a major challenge was the adjustment of a suitable solvent mixture, arising from the differences in solubility of GGM and the activated fatty acids. A mixture of DMSO and THF showed to be suitable and the esterifications were performed in homogeneous conditions using imidazole as a catalyst. Different amounts of activated fatty acids were used in distinguished reactions resulting in GGM-*grafted*-fatty acids with different degrees of substitution of the GGM. In order to remove unreacted fatty acid and imidazole from the product, the reaction mixture was precipitated in ethanol. After filtration, the precipitate was dispersed in deionized water and transferred into dialysis tubes in order to remove solvent residues from the GGM derivatives. Hereby the material was partially dissolved and a water-soluble and a water-insoluble fraction were collected separately. The degree of substitution of the GGM-*grafted*-fatty acid was determined by ^1H NMR and in Figure 8 the spectra of GGM and its GGM-*grafted*-C9 products are shown exemplary.

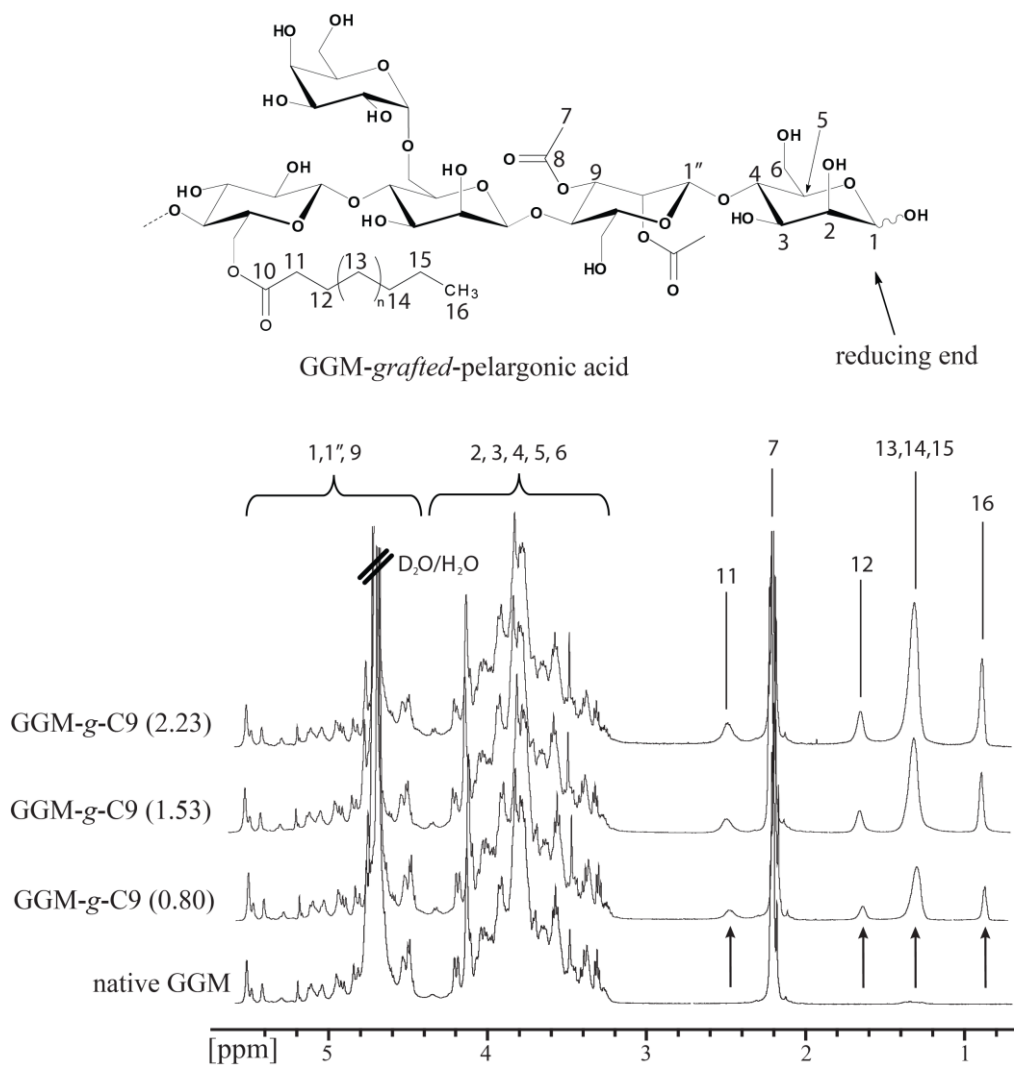


Figure 8. ^1H NMR spectra of native GGM and the esterification products of GGM and pelargonic acid. The labelling of the GGM derivatives includes “g” for grafted and the label of the used fatty acid (C9, C14 or C18). The number in parentheses represents the number of fatty acid chains introduced to the GGM chain. For all the samples D_2O was used as solvent and the acetyl peak was used to calibrate the spectra.

In the NMR spectra of GGM and the GGM-g-C9 derivatives the region from 4.6 to 5.5 ppm includes the anomeric protons (H-1 and H-1’’) of the sugar units of GGM, as well as the proton located close to an acetyl group (H-9) (Hannuksela & Hervé du Penhoat, 2004). The CH_3 -group (H-7) of the acetyl groups gave signals in the region between 2.11

and 2.28 ppm. The peak at 0.88 ppm belongs to the protons of the terminal CH₃-group of the fatty acid chain (H-16), and the peak at 1.31 ppm belongs to the CH₂ groups (H-13, 14, 15) of the fatty acid. The CH₂-groups close to the carbonyl-function H-11 and H-12 gave separated signals at 2.49 and 1.66 ppm, respectively. Due to the complexity of the GGM spectrum, it was not possible to define which position (C2, C3, or C6) was preferred during the esterification reactions. The growth of the intensity of the individual peaks of the fatty acids in the ¹H NMR spectra visualizes an increasing degree of substitution of GGM. The exact DS value for the different GGM-*grafted*-fatty acid products was determined after calibration of the ¹H NMR spectra (see chapter 3.2.3 for detailed information about the calibration of the ¹H NMR spectra) by determining the integration value for the fatty acid CH₃-group signal at 0.88 ppm. The DS values for all the GGM-fatty acid derivatives are listed in Table 1.

Table 1. Results of the esterification and reductive amination reactions of GGM with three different fatty acids (C9, C14 and C18). Some of the reactions resulted in a water soluble and water insoluble fraction, which are listed separately.

Product ^a	Molar ratio		M _n [Da] ^b	M _w /M _n ^b	DS ^c
	GGM:fatty acid	Yield [%]			
Water soluble					
GGM	-	-	6057	2.76	-
GGM-g-C9 (0.80)	1:2	34	6382	2.14	0.029
GGM-g-C9 (1.53)	1:4	25	6821	2.14	0.055
GGM-g-C9 (2.23)	1:8	30	7328	1.91	0.08
GGM-g-C14 (0.82)	1:2	31	6945	1.96	0.029
GGM-g-C14 (1.14)	1:4	16	6067	2.07	0.041
GGM-g-C14 (1.95)	1:8	15	7288	1.66	0.07
GGM-g-C18 (0.68)	1:2	35	6744	2.3	0.024
GGM-g-C18 (1.07)	1:4	30	7191	2.02	0.038
GGM-g-C18 (1.42)	1:8	34	8804	2.02	0.051
GGM- <i>b</i> -C9	1:5	45	6036	2.43	-
GGM- <i>b</i> -C14	1:5	57	6769	2.68	-
GGM- <i>b</i> -C18	1:5	35	6679	2.15	-
Water insoluble					
GGM-g-C9 (4.85)	1:8	5	12775	1.79	0.173
GGM-g-C14 (2.51)	1:2	19	9084	2.11	0.09
GGM-g-C14 (3.13)	1:4	18	10372	1.95	0.112
GGM-g-C14 (5.45)	1:8	21	10978	1.95	0.195
GGM-g-C18 (1.68)	1:2	8	7769	2.2	0.06
GGM-g-C18 (3.42)	1:4	30	9436	1.85	0.122

^aIn brackets are the average numbers of fatty acid per GGM chain in the final products;

^bMolar mass determination after acetylation of the GGM and the GGM derivatives (procedure in “HPSEC” in the experimental section); ^cDegree of substitution (with maximum DS being 3).

A logical trend of the GGM-*grafted*-fatty acid derivatives of being less water-soluble the higher the DS value and the longer the fatty acid chain (from C9 to C18) could be assessed. The relatively low yields in which the products were collected, were assumed to

be due to the formation of EtOH soluble aggregates during the precipitation process. Higher DS values than the one reported in table 1 have been reported for the esterification of cellulose under similar reaction conditions (Hussain et al., 2004). Hence it is likely, that EtOH soluble GGM derivatives were formed during the esterification. These products were not collected with the applied purification method.

The GGM-*grafted*-fatty acid derivatives were obtained as mixtures and so for example the product GGM-*g*-C9 (2.53) might contain unmodified GGM, as well as GGM grafted with four fatty acids. In order to obtain amphiphilic GGM-fatty acid derivatives with a defined structure, another approach had to be chosen. Each native GGM chain contains exactly one reducing end aldehyde group, which is available for chemical modification with for example amino functional reactants in a reductive amination. In this work, the previously activated fatty acids were converted with BOC-protected ethylenediamine and consecutively reacted with GGM in a solvent mixture of EtOH and DMSO applying sodium cyanoborohydride as a reducing agent. The final GGM-*block*-fatty acid derivatives could be purified after the reaction, similar to the GGM-*grafted*-fatty acids. A precipitation in EtOH followed by a dialysis against de-ionized water and freeze-drying were performed, resulting in residue free products. The successful conversion of all the reducing end groups of GGM, and hence the proof that a homogeneous and pure product was obtained, was verified by ^1H and ^{13}C NMR (Figure 9).

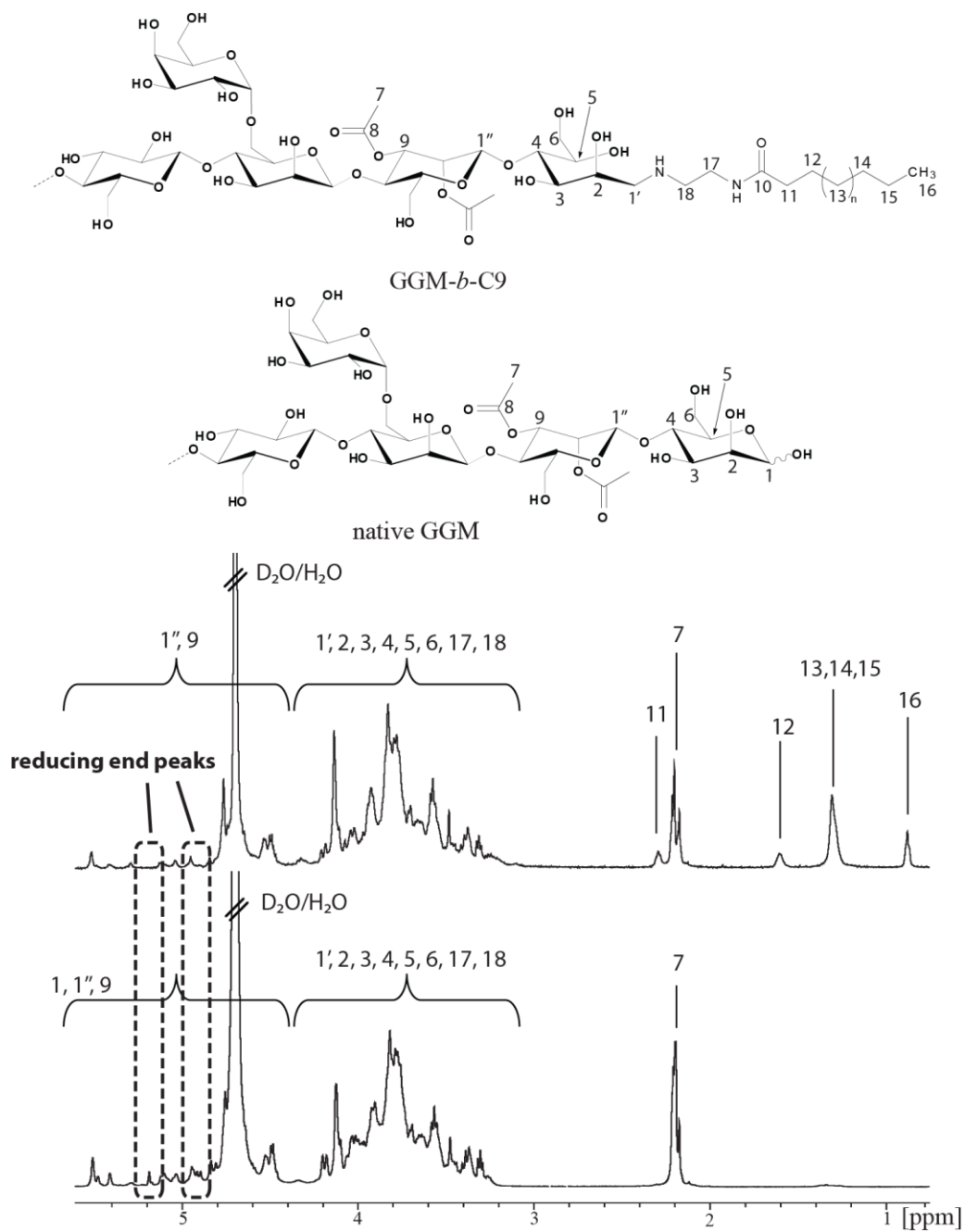


Figure 9. ¹H NMR spectra of GGM (bottom) and GGM-block-pelargonic acid (D₂O as solvent). In the dashed rectangles the disappearance of the mannose reducing end peak can be seen.

In Figure 9, the ^1H NMR spectra of GGM and its block-structured derivative with pelargonic acid as a hydrophobic tail is shown. The peaks of GGM and the fatty acid were assigned in the same way as described above for the esterification products. The protons of the CH_2 -groups (H-17 and H-18) of C9-NH₂ overlap with the signals of GGM in the peak region between 3.2 and 4.4 ppm and could not be assigned separately. The complete conversion of the reducing end was verified by the complete disappearance of the reducing end signals of GGM at 4.93 ($\alpha\text{-Manp}^{\text{R}}$) and 5.20 ppm ($\beta\text{-Manp}^{\text{R}}$) (dashed rectangles in Figure 9). While the reducing end peaks of GGM disappear in the GGM-*block*-fatty acid derivative spectra, the signals of the corresponding fatty acid chains appear. The CH_3 signal at 0.88 ppm was used to confirm the presence of exactly one fatty acid in each macromolecule and was found to be exactly three (meaning one CH_3 group) at full conversion of the GGM reducing end. In order to confirm the complete conversion of all the reducing end units, including all the reducing end glucose units, ^{13}C NMR measurements were performed (Figure 10).

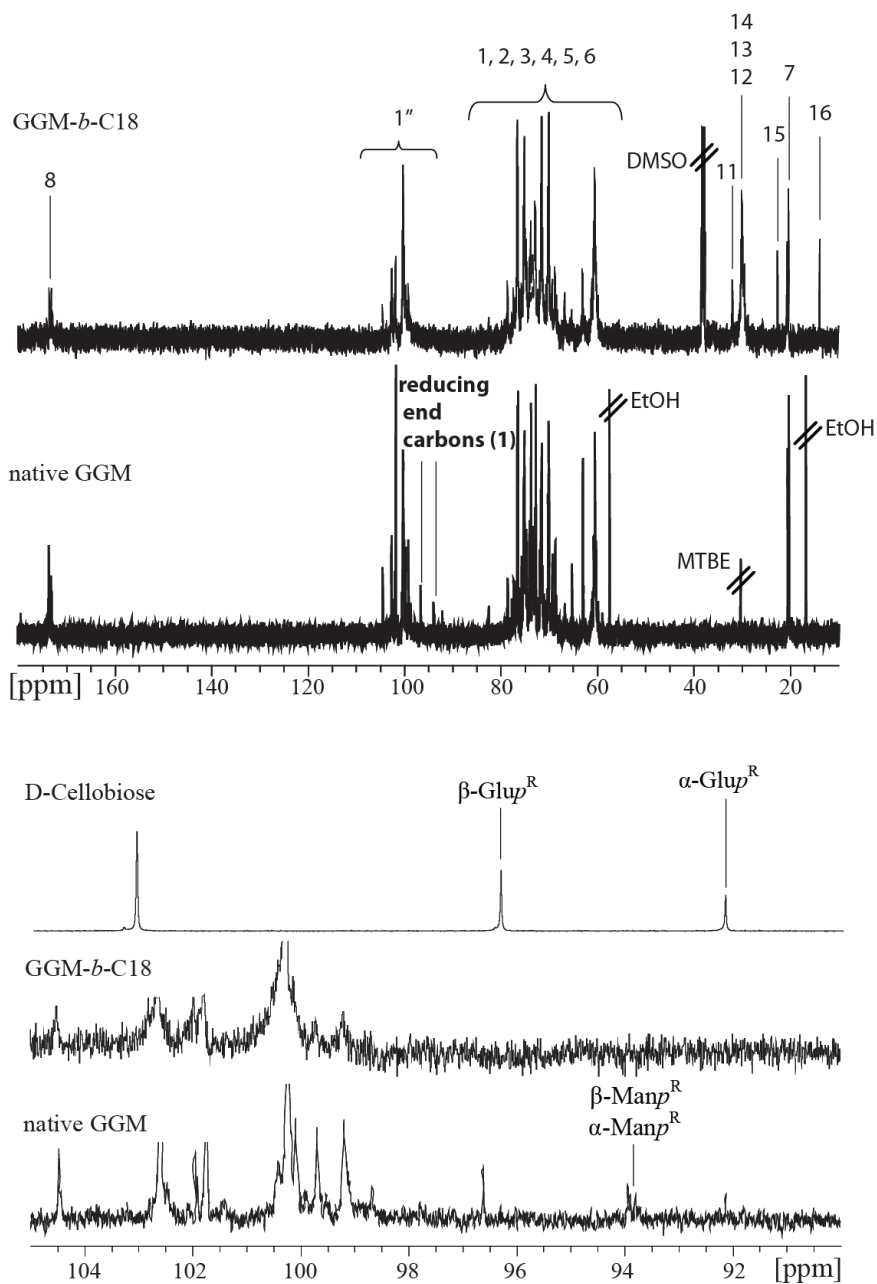


Figure 10. ^{13}C NMR spectra of native GGM in D_2O and the GGM-block-C18 derivative in $\text{DMSO-}d_6$ (top) and the amplification of the reducing end signals (bottom). The peak numbering is the same as in Figure 9.

In the ^{13}C NMR spectra of the native GGM and its block-structured fatty acid derivative the appearance of supplementary signals for the modified GGM in the peak region from 14.11 to 31.88 ppm could be observed. The $\alpha\text{-Manp}^{\text{R}}$ and $\beta\text{-Manp}^{\text{R}}$ of the native GGM have a chemical shift of 94.86 and 94.72 ppm, respectively, assigned in a previous work (Hannuksela & Hervé du Penhoat, 2004). To correctly assign the peaks at 92.11 and 96.82 ppm, a spectrum of cellobiose was recorded. By comparing the spectra of cellobiose and native GGM, the signal at 92.11 ppm was assigned to $\alpha\text{-Glup}^{\text{R}}$, and the signal at 96.82 ppm was assigned to $\beta\text{-Glup}^{\text{R}}$. All the signals of the reducing end carbons completely disappeared in the spectra of the block-structured GGM derivatives proofing the successful conversion of all the GGM reducing ends during the reaction. The GGM-*block*-fatty acid derivatives were all readily soluble in water and gave light brownish-coloured solutions.

It could be shown that fatty acids are possible starting reagents for the chemical modification of GGM resulting in amphiphilic bio-based materials. Two different product groups could be prepared separately and were analysed in detail by ^1H and ^{13}C NMR. All the water-soluble GGM-fatty acid derivatives were assumed to be potential surfactants and were tested in respect to their ability to lower the surface tension in water (section 5.3.1) [I]. Furthermore, the GGM-*block*-structured derivatives were examined as hydrophobizaion agent for the surface modification of NFC (section 5.3.2) [III].

5.2.2 *Block-copolymers of GGM and PDMS [III]*

Beside the application of fatty acids as a hydrophobic tail [I], also polydimethylsiloxane (PDMS) was attached to GGM at its reducing end. Several hydrophobic synthetic polymer chains have been coupled to water soluble polysaccharides, such as polystyrene (Bosker et al., 2003; Loos & Stadler, 1997), polyesters (Liu & Zhang, 2007) or siloxanes (Halila et al., 2008). These well-defined copolymers were proved to have very interesting properties such as self-assembly (Houga et al., 2008) and to find a potential application as surfactant (Halila et al., 2008). In this work, reductive amination was chosen as an easier reaction compared to the described application of “click”-chemistry (Halila et al., 2008) for the introduction of PDMS to the GGM chain. PDMS is known for being highly hydrophobic and is used in large scale for the production of additives for paints and coatings. PDMS is usually produced by living anionic polymerization of D_3 using a organolithium reagent as initiator (Elkins & Long, 2004) and is commercially available in different molar masses and with distinguished end functionalities, such as epoxides or amines. For the performed experiments, a diamino terminated PDMS ($\text{NH}_2\text{-PDMS-}$

NH₂) with a molar mass of 900 Da was applied for the synthesis of block-structured AB and ABA copolymers (Figure 11).

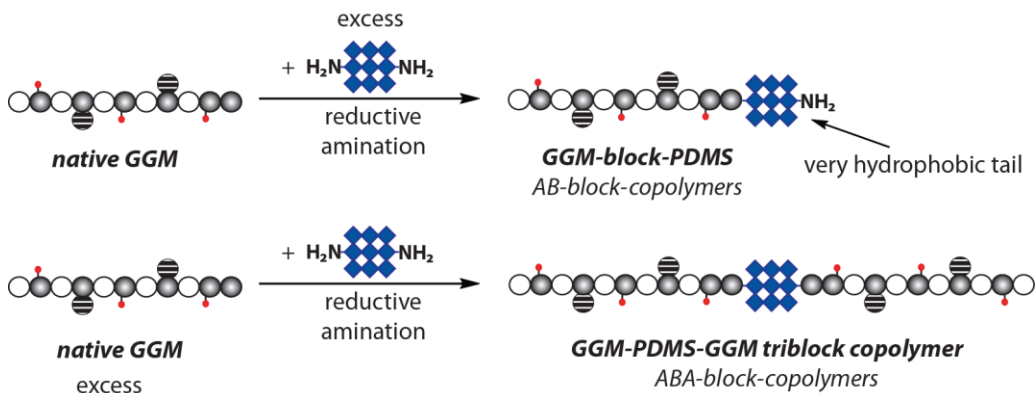
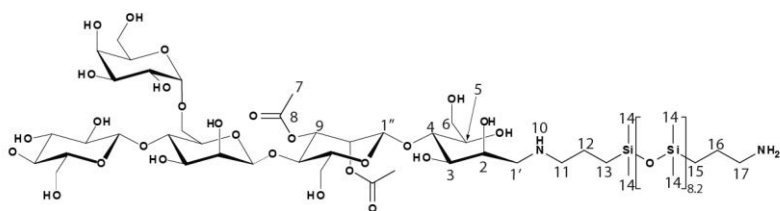
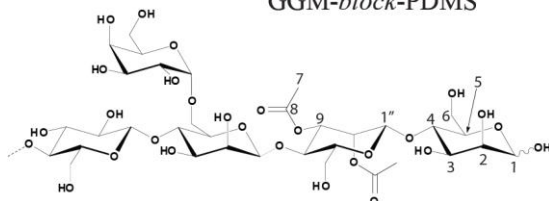


Figure 11. Schematic illustration of the synthesis of GGM-block-PDMS and GGM-PDMS-GGM triblock copolymers.

For the synthesis of defined AB-structured derivatives, a 20-fold excess of the difunctional NH₂-PDMS-NH₂ was used in order to assure that no ABA-structured products were formed. For the synthesis of the ABA-structured GGM-PDMS-GGM derivative an excess of GGM was applied to assure the complete conversion of all the amino groups of the functional PDMS. The reaction conditions for the reductive aminations were similar to the ones used for the GGM-*block*-fatty acid derivatives with the main difference that a THF/DMSO solvent mixture was used. The excess of GGM was after precipitation of the reaction mixture removed by dialysis during which the formed ABA-structured GGM-PDMS-GGM derivatives remained in the dialysis tube whereas the unreacted GGM migrated into the surrounding water. The successful preparation of the respective GGM derivative was confirmed by ¹H NMR and COSY spectra (Figure 12a and 12b).



GGM-block-PDMS



native GGM

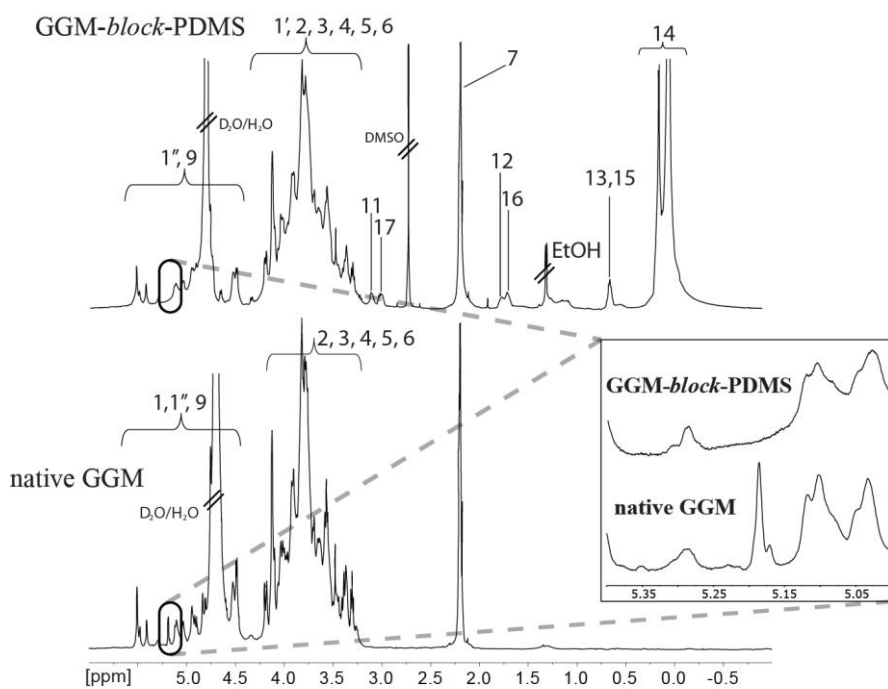


Figure 12a. ^1H NMR spectra of native GGM and its block-structured derivative recorded in D_2O . In the insert the reducing end peak region of GGM is highlighted and the complete disappearance of the reducing end peak at 5.17 ppm can be observed for the GGM-block-PDMS.

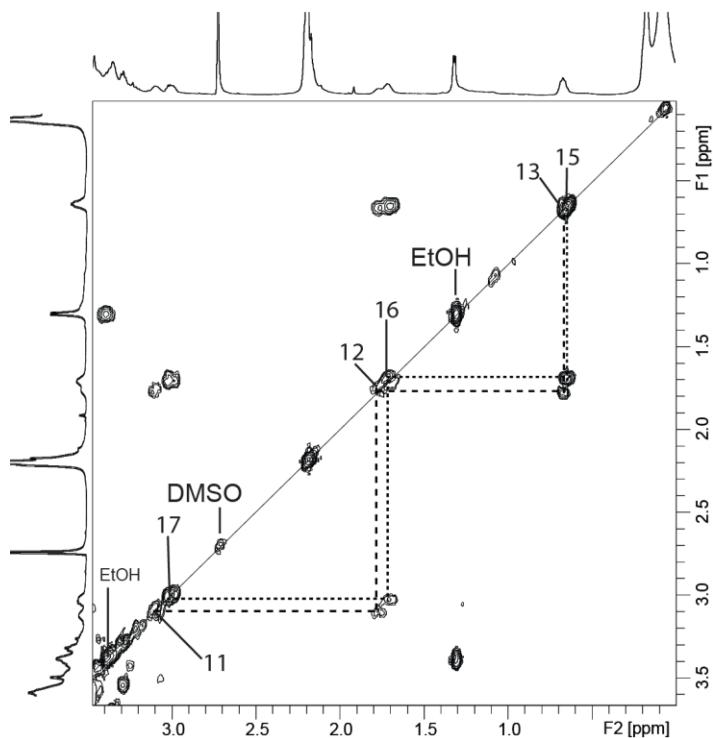


Figure 12b. COSY spectrum of GGM-*block*-PDMS.

The GGM-*block*-PDMS derivative was analysed by ^1H NMR and the full conversion of the reducing end peak of GGM at 5.20 ppm could be observed (Figure 12a). At the same time the characteristic peaks of the PDMS CH_3 groups in the range from -0.18 to 0.23 ppm emerged. In the final product, two distinguished alkyl chains were present, originating from the NH_2 -PDMS- NH_2 . To correctly assign the respective signals in the ^1H NMR spectra, the CH_2 (H-11) group in the neighbourhood of the -NH- was identified to be at 3.12 ppm. This identification was performed by recording a ^1H NMR of a GGM-PDMS-GGM derivative in which all the amino groups of NH_2 -PDMS- NH_2 had reacted and hence only -NH- CH_2 - was present, whereas in the GGM-*block*-PDMS derivative there was one -NH- CH_2 - and one NH_2 - CH_2 - group with similar shifts in the ^1H spectrum. The CH_2 (H-17) signal next to the unreacted NH_2 was assigned to the peak at 3.01 ppm. By evaluating a 2D COSY spectrum of GGM-*block*-PDMS the Si- CH_2 - CH_2 - CH_2 -NH- (H-12) signal was found to be at 1.77 ppm and the Si- CH_2 - CH_2 - CH_2 - NH_2 (H-16) at 1.71 ppm. The CH_2 groups next to the Si atoms had a similar shift of 0.56 for Si- CH_2 -(CH_2) $_2$ -NH- (H-13) and 0.55 ppm for Si- CH_2 -(CH_2) $_2$ - NH_2 (H-15). The acetyl groups (H-7) of GGM could be found at 2.09 ppm. Here it has to be noted that during

the chemical modification of GGM, no deacetylation took place. For further confirmation for the formation of the desired products, FTIR spectra were also recorded (Figure 13).

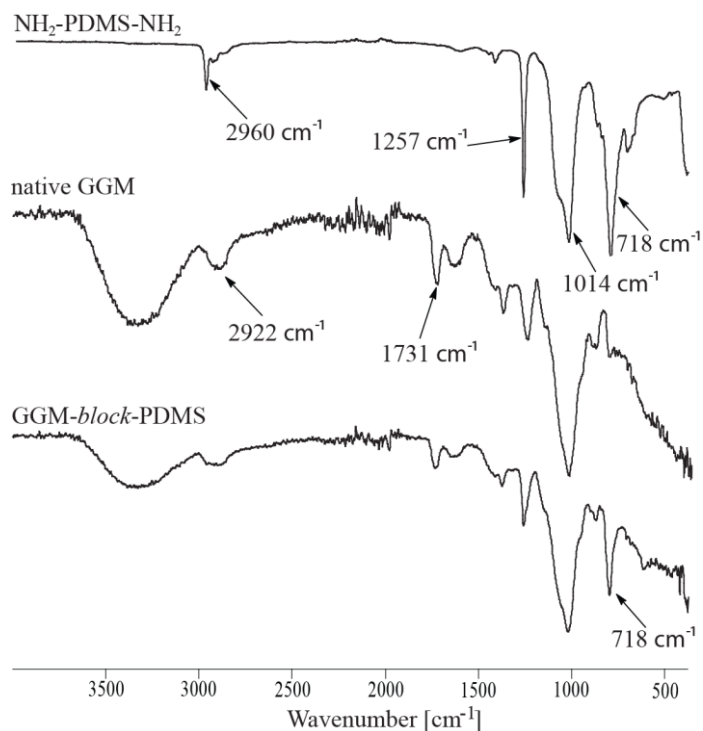


Figure 13. FTIR spectra of the reagent $\text{NH}_2\text{-PDMS-NH}_2$ native GGM and GGM-*block*-PDMS.

The spectrum from $\text{NH}_2\text{-PDMS-NH}_2$ (Figure 13) was recorded as a reference and at 2960 cm^{-1} , the C-H valence vibration signal could be detected (Cai et al., 2010). The C-H bending vibration was assigned to the signal at 1257 cm^{-1} and the Si-O valence vibration was found at 1014 cm^{-1} . Furthermore, the Si-C valence vibration could be separately detected at 718 cm^{-1} . The latter peak is the one that could also be observed in the spectrum of GGM-*block*-PDMS, which tightens the proof of the successful formation of the product. The other signals resulting from the PDMS chain in the GGM derivative could not be separately assigned because they were overlapping with signals originating from the GGM chain. The carbonyl group signal ($\nu_{\text{C=O}}$) at 1731 cm^{-1} is present in the native GGM spectrum, as well as in the GGM-*block*-PDMS arising from the acetyl group. Beside the spectroscopic analysis of the GGM-*block*-structured PDMS derivatives, also size exclusion measurements were performed following a similar approach as described

earlier for the GGM-*block*-fatty acid derivatives using THF as an eluent (unpublished results). Therefore, native GGM, GGM-*block*-PDMS, and GGM-PDMS-GGM were hydrophobized using acetic anhydride. The acetylated GGM revealed a number-average molar mass of 6.4 kDa and the NH₂-PDMS-NH₂ had a molar mass of 0.9 kDa. The M_n value for the GGM-*block*-PDMS was with 7.8 kDa, slightly higher than the theoretical value of 7.3 kDa. For the ABA-structured GGM-PDMS-GGM derivative a M_n value of 13.7 kDa was determined what corresponds exactly to the theoretical value and confirmed the results of the NMR spectra. Overall the successful synthesis of GGM block-structured derivatives was reported and the AB-structured derivatives were further tested with respect to their applicability for the hydrophobization of cellulose surfaces (section 5.3.2). The ABA-structured derivatives have in this study not been evaluated in applications and were only needed for the analytical part.

5.2.3 **Functional GGM-*block*-structured derivatives by SET-LRP [II]**

In the previously described GGM derivatizations hydrophobic groups were introduced to the GGM main chain by esterification of the hydroxyl groups or by reductive amination of the reducing end of GGM. The resultant GGM derivatives revealed amphiphilic structures and were successfully tested for the reducing of the water surface tension and the surface modification of NFC. However, the utilized synthesis path had some limitations. On the one hand the chain length of the attached chain was restricted by the applied starting material (e.g. fatty acids with either 9, 14 or 18 carbons) and on the other hand only hydrophobic properties were introduced to the GGM chain. In order to extend the possibilities to produce GGM block-structured derivatives containing synthetic polymer chains with distinguished chemical and physical features, another synthesis approach had to be chosen. The *in situ* polymerization of monomers with specific characteristics has shown to be a powerful approach for the development of novel GGM grafted copolymers (Voepel et al., 2011b), as well as for the formation of block-structured copolymers of other polysaccharides such as dextran (Houga et al., 2007). In this work, firstly an amino functional initiator was prepared by combining two previously described approaches (Sadhu et al., 2004; Zhang et al., 2011) [II] (Figure 14).

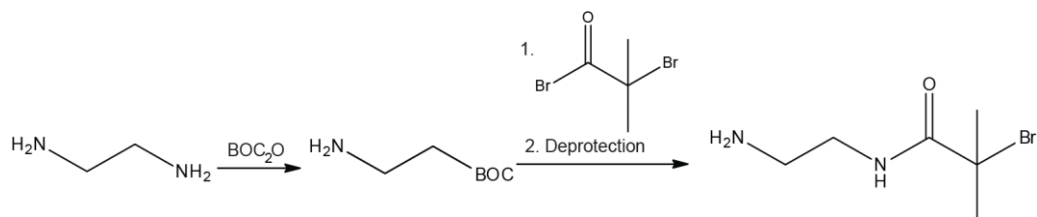


Figure 14. Synthesis of an amino functional initiator using ethylenediamine as a starting material.

In Figure 14 is shown that the amino functional initiator was produced in a three steps reaction in which in a first step one amino group of ethylenediamine was protected using BOC₂O and then consecutively converted with BIBB in an esterification. In a last step, the amino group was deprotected using HCl gas and was ready to be applied in a reductive amination with GGM. The reductive amination was performed as described earlier (section 5.2.1), but deionized water could be used as a solvent because all the reactants were well soluble at pH 4. Several reactions were performed in order to determine the minimum amount of the amino functional initiator needed, because its synthesis was quite tedious and time consuming. The end functionalized GGM macroinitiator was analysed by ¹H and ¹³C NMR in order to confirm the complete conversion of the reducing end of GGM (Figure 15).

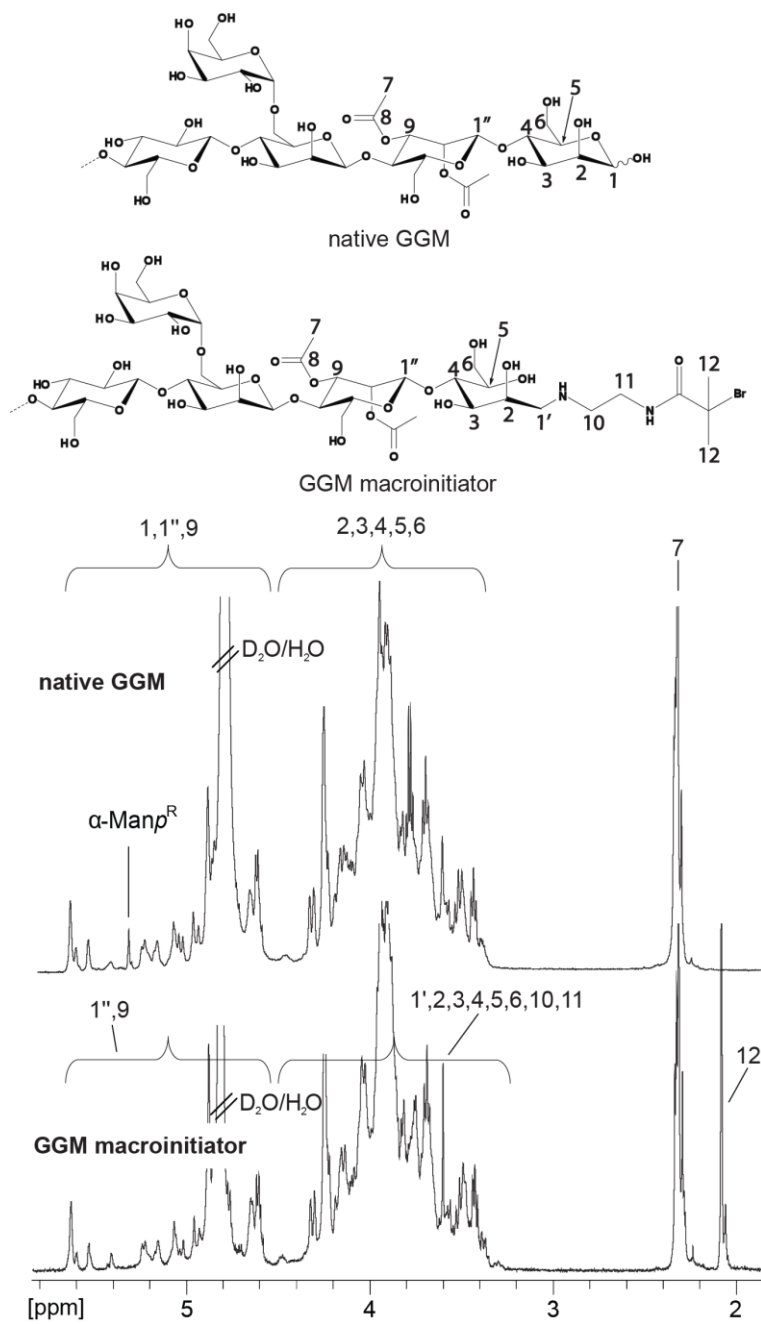


Figure 15. ^1H NMR spectra of native GGM and the monofunctional GGM macroinitiator recorded in D_2O at 35°C .

In the spectra of the GGM macroinitiator (Figure 15) the CH₃-groups (H-12) in the neighbourhood of the bromine gave signals from 1.91 to 1.97 ppm and corresponded to six protons. These signals were used for the quantification of the functionalization of GGM and in the recorded ¹H NMR spectra of the screening reactions a simultaneous decrease of the reducing end peaks of GGM could be assessed when more BIBB was introduced to GGM (Figure 16).

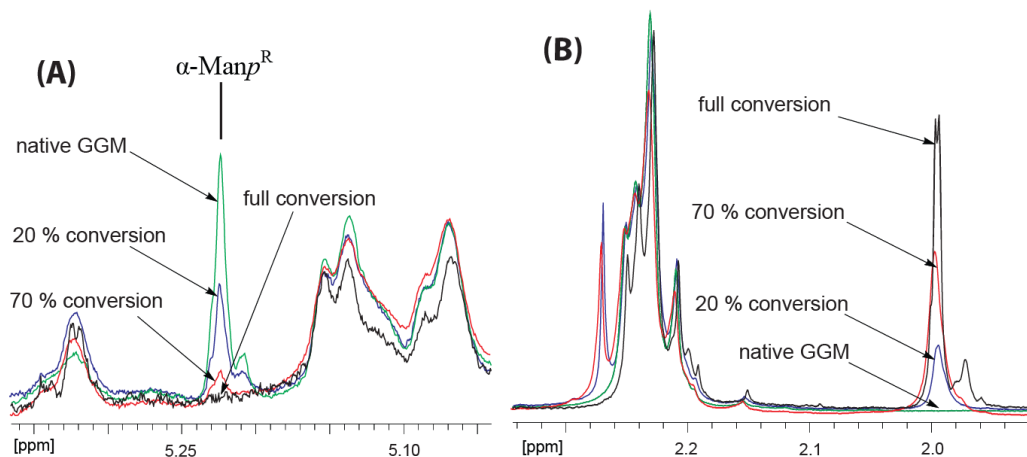


Figure 16. Insert of the ¹H NMR spectra for different conversions of the mannose reducing end peak (α -Manp^R) (A) and the CH₃-groups from the α -bromoisobutyryl group (B).

In Figure 16, an amplification of the GGM reducing end peak region (A in Figure 16) and the CH₃ peak region (B in Figure 16) are highlighted. For the native GGM the distinct mannose reducing end peak could be detected which decreased continuously while more initiator groups were introduced to GGM. It was found that a 6-fold excess of the amino functional initiator was sufficient to assure a full conversion of the GGM reducing ends and pure GGM macroinitiator was obtained. The GGM macroinitiator was consecutively applied in a controlled polymerization using three different monomers. The selected monomers were able to build up polymer chains with distinguished characteristics. So the polymerization of MMA results in amphiphilic GGM copolymers and the co-polymerization with NIPAM in pH and temperature sensitive polymers. When MeDMA was used as a monomer, block-structured copolymers were formed in which the synthetic polymer chain contained high amounts of charges (Figure 17).

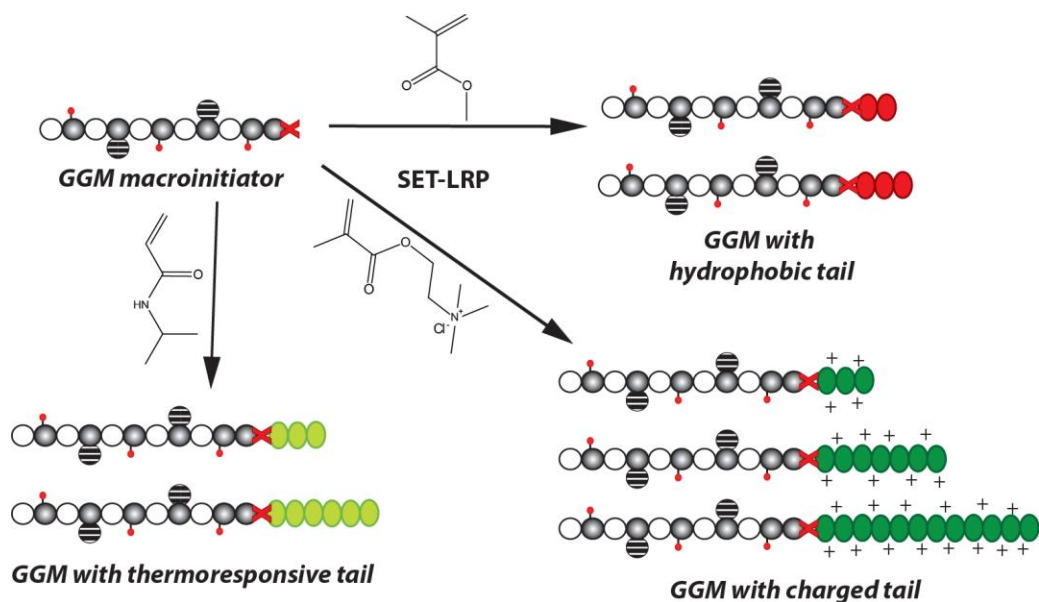


Figure 17. Schematic illustration of GGM block-structured copolymers containing synthetic polymer chains with distinguished properties and different molar masses.

The main aim of this work was the synthesis of GGM block-structured copolymers in which the synthetic polymer chains had distinguished physical properties and a defined chain length [II]. In order to tailor the chain length of the synthetic polymer, a controlled polymerization had to be applied. Single electron transfer-living radical polymerization (SET-LRP) has been reported to be a suitable polymerization method for the derivatization of polysaccharides in water or other polar solvents or solvent mixtures (Edlund & Albertsson, 2012; Zoppe et al., 2010). For the polymerization of MeDMA and NIPAM a DMSO/water mixture was used as solvent, whereas for MMA pure DMSO was used. The solvents were freshly distilled under argon prior use in order to remove all oxygen traces, which could be harmful during the SET-LRP. As a copper source metallic copper pieces were used and as ligand Me₆-Tren was applied. The polymerizations were carried out in Schlenk tubes under argon and 40 °C. After 30 h the polymerization products were recovered by precipitation in EtOH and purified by dialysis. The success of the polymerization was confirmed by ¹H NMR and HPSEC. The molar mass determination by HPSEC showed that GGM-*block*-copolymers with different chain lengths could be prepared using the three selected monomers (Table 2).

Table 2. Reaction conditions for the polymerizations and the molar masses determined by ^1H NMR and HPSEC measurements.

monomer	[M]/[I] ^a	$M_{n, \text{theo.}}^b$ (Da)	$M_{n, \text{NMR}}^c$ (Da)	SEC	
				M_n (Da)	M_w/M_n
MeDMA	9	6750	-	8400 ^d	1.32 ^d
MeDMA	24	9750	5500	9200 ^d	1.73 ^d
MeDMA	193	44750	21300	50000 ^d	1.61 ^d
MMA	10	5750	5500	5200 ^e	1.52 ^e
MMA	20	6750	5600	6600 ^e	1.72 ^e
MMA	50	9750	5800	8100 ^e	2.70 ^e
MMA	100	14750	6700	11400 ^e	2.78 ^e
NIPAM	44	9750	5800	14300 ^e	1.99
NIPAM	96	15610	9600	16900 ^e	1.95

^a monomer (*M*) to GGM macroinitiator (*I*) ratio. ^b theoretical molar mass of the GGM derivatives after polymerization (does not take conversion into account): $M_{n, \text{theo.}} = (([M]/[I]) \times (\text{molar mass monomer}) + (\text{molar mass GGM}))$. ^c molar mass of the products determined by ^1H NMR. ^d HPSEC results using 0.1 M NaNO₃ solution as eluent. ^e HPSEC results using THF as eluent ($M_{n, \text{cal}}$).

It has to be noted that the polydispersities of the copolymers were rather high (up to 2.8) for GGM-*block*-pNIPAM and GGM-*block*-pMAA, indicating unwanted recombination during the polymerization. The potential recombination of the active polymer chains was assumed to be due to formation of micelles in the reaction solution. However, for the GGM-*block*-pMeDMA the polydispersity was sufficiently low (<1.7) to prove the controlled character of the polymerization. Overall it can be summarized that GGM is a suitable starting material for the synthesis of block-structured copolymers with different functionalities and defined molar masses. In this work the focus was put on the potential synthesis of the distinguished GGM block-structured derivatives and no application testing was carried out, due to the low amounts of material produced. Anyhow, the results of this work represent a strong basis for further research and could allow the implementation of GGM in various applications.

5.2.4 GGM-based hydrogels [IV]

In the previous chapters the synthesis of GGM containing different functional groups was described. Hereby the GGM was either derivatized by modifying its hydroxyl groups or the reducing end resulting in mostly soluble products. In this section, the production

pathway for GGM-based hydrogels will be elaborated, for which firstly a GGM macromonomer was produced by transesterification and subsequently a free radical polymerization was performed (Figure 18) [IV].

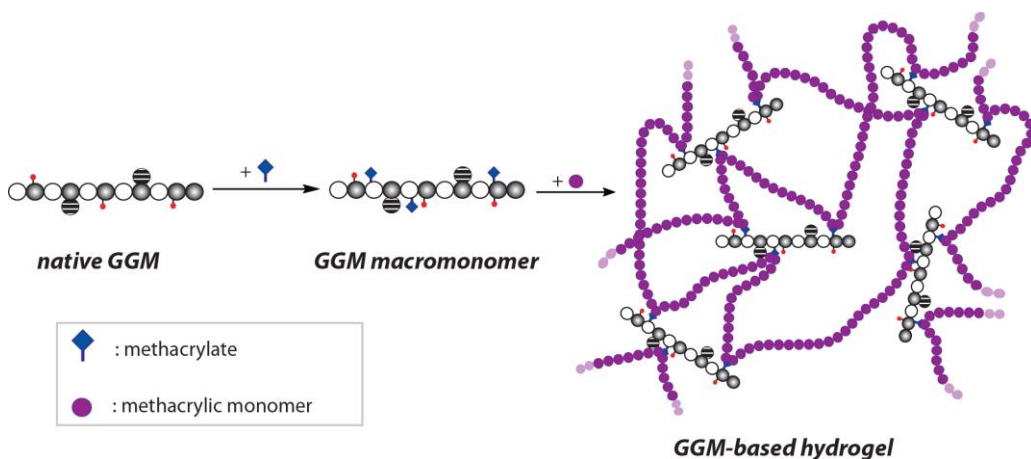


Figure 18. Transesterification of GGM by glycidyl methacrylate using DMAP as a catalyst and the consecutive hydrogel synthesis.

Hydrogels are by definition polymeric networks, which are able to swell in water and are used in various applications ranging from food over drug delivery to wound healing composites (Vashist et al., 2014). The target of this work was the removal of toxic ions from aqueous solutions and hence the potential application of the GGM-based hydrogels in water purification systems.

The GGM macromonomers were obtained after transesterification of GGM with glycidyl methacrylate by adapting a previously reported method using DMAP as a catalyst (Peng et al., 2012a). DMSO and DMF were tested as solvents and the reaction temperature was set to 50 °C. After 16 h the reaction mixture was transferred into dialysis tubes and the solvent, DMAP, the excess of GMA, as well as the formed glycidol were removed. The purified GGM macromonomers were obtained after freeze-drying and were analysed by ^1H NMR and ^{13}C NMR. For the quantification of the methacrylic groups introduced into the GGM main chain, the ^1H NMR spectra of the different products were analysed (Figure 19). For this work two different GGMs were used having number-average molar masses of 4.8 and 21.5 kDa and the methacrylic derivatized GGMs were labelled GGM5-MA and GGM22-MA, respectively.

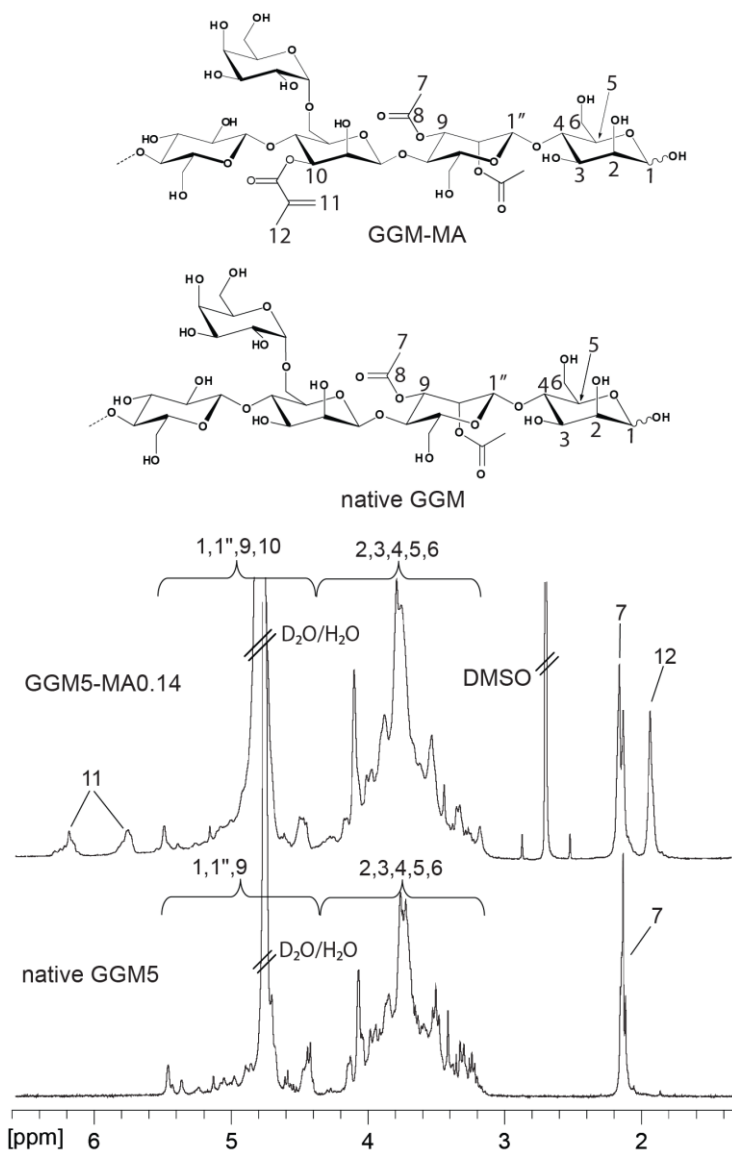


Figure 19. ^1H NMR spectra of native GGM (GGM5) and a GGM5-MA crosslinker (GGM5-MA0.14) in D_2O .

All the GGM-MA derivatives were readily soluble in water and were dissolved in D_2O for the NMR measurements. In the spectrum of the GGM5-MA0.33, three additional peak areas could be identified. The CH_3 groups (H-11) of the methacrylate attached to GGM gave signals from 1.81 to 2.06 ppm. The two protons on the unsaturated carbon

(H-12) gave signals in the regions 5.70-5.91 and 6.09-6.38 ppm. The DS_{MA} for the different GGM-MA derivatives was determined using the integration value of the peak area from 1.81 to 2.06 ppm as a reference. In the labelling of the GGM macromonomers, the number in the end indicates the degree of substitution (DS_{MA}) of the GGM derivatives. In Table 3 an overview of the produced GGM-MA derivatives is given and the DS_{MA} , as well as the number of MA groups incorporated in one GGM chain are listed.

Table 3. Reaction conditions for the transesterification of glycidyl methacrylate (GMA) with GGM.

Crosslinker	T [°C]	GMA/X ^a	DMAP ^b	Solvent	MA per GGM chain ^c	DS_{MA}
GGM5-MA0.04	50	5:7	5	DMF	0.97	0.03
GGM5-MA0.25	50	5:7	10	DMF	6.89	0.25
GGM5-MA0.32	50	5:7	20	DMF	8.87	0.32
GGM5-MA0.03	50	5:7	10	DMSO	0.87	0.03
GGM5-MA0.14	50	5:7	20	DMSO	3.78	0.14
GGM5-MA0.33	50	10:7	20	DMSO	9.23	0.33
GGM22-MA0.41	50	5:7	20	DMF	50.78	0.41
GGM22-MA0.32	50	5:7	20	DMSO	39.7	0.32
GGM22-MA0.20	50	2.5:7	20	DMSO	24.7	0.20

^a Molar ratio of GMA to anhydrous sugar units of GGM; ^b wt.-% of catalyst in respect to GGM; ^c Average amount of MA groups present in each GGM chain.

It was found that the DMF is a better solvent for the transesterification and slightly higher DS_{MA} values could be reached compared to DMSO when the same amount of catalyst and the same ratio of GGM and DMA were used. A logical trend of an increasing DS_{MA} was determined when larger amounts of catalyst and GMA were applied.

The synthesized and purified GGM-MA derivatives were subsequently used as a crosslinking agent in the synthesis of GGM-based hydrogels. Therefore, GGM-MA was dissolved in deionized water and mixed with MeDMA as a monomer. After the addition of defined amounts of ammonium persulfate as an initiator, the dissolved oxygen was removed by bubbling nitrogen into the reaction solution and then the closed reaction tube was placed in an oil bath at 75 °C. After 2 h the reaction was stopped by mixing the formed gel with an excess of deionized water in order to remove all soluble polymer chains, which had not been attached to the network. Then the hydrogels were oven-

dried, grinded, and their swelling rate was determined by placing 100-200 mg of material in an excess of deionized water for 24 h (Table 4).

Table 4. Swelling rate (Q) for different GGM-based hydrogels.

Hydrogel composition	Q
[GGM5-MA0.14;10;10;5]	57.6
[GGM5-MA0.14;20;10;5]	68.6
[GGM22-MA0.20;20;7;1]	26.6
[GGM22-MA0.20;20;10;5]	18.4
[GGM22-MA0.32;20;10;5]	6.6

In Table 4, the swelling rates of five selected hydrogels are listed and for the product [GGM5-MA0.14;10;10;5]. This means, for example, that the dried material could absorb 57.6 times its own weight in water. These values are comparable to the ones reported for similar polysaccharide-based hydrogels (Peng et al., 2011). The labelling of the samples is given in the experimental part. For the hydrogels [GGM5-MA0.14;20;10;5] and [GGM22-MA0.20;20;10;5], low M_n and high M_n GGM-MA derivatives were used, for which the DS_{MA} was comparable. All the other parameters during the hydrogel synthesis were the same (same amount of initiator and monomer) and it could be observed that for the GGM5-MA derivative the swelling rate was 3.7 times higher than that of the GGM22-MA derivative. Because the GGM22-MA contained more than 6 times more MA groups per molecule, denser networks were formed compared to the GGM5-MA with a similar DS_{MA} . When using GGM22-MA with a DS_{MA} of either 0.20 or 0.32 for the hydrogel synthesis with equal amounts of initiator and monomer ([GGM22-MA0.20;20;10;5] and [GGM22-MA0.32;20;10;5]), the swelling rate for the GGM22-MA0.32 based hydrogel was 2.7 times lower than that for the GGM22-MA0.20 one. This is logical, because GGM22-MA0.32 contains more MA groups and hence is the more efficient crosslinker. This leads to a denser network formation with shorter polymer chains and hence to a reduced swelling potential. One hydrogel with a smaller amount of GGM-MA and smaller amount of initiator was produced ([GGM22-MA0.20;20;7;1]). It could be observed that the swelling rate was increasing compared to [GGM22-MA0.20;20;10;5] due to the smaller amount of radicals in the solution. This led to the formation of longer polymer chains, which in combination with a smaller amount of crosslinking points resulted in a less dense network.

In Figure 20, a series of photographs of [GGM5-MA0.14;20;10;5] illustrates the swelling process of the GGM-based hydrogels. At $t = 0$, the hydrogel was water-free after oven drying and showed a brownish colour, which likely arose from the synthetic polymer. After merging the solid hydrogel into a large excess of water, it started swelling and it could be observed that after 10 min the brown colour vanished in the outer area of the sample. After 120 min the hydrogel had taken up around 15 times the amount of water with respect to its initial weight. It could also be seen that up to that moment the physical consistency of the hydrogel was stable and only a light yellow stain was left in the core of the structure. After 22 h the hydrogel was fully swollen ($Q = 68.6$) and broke into smaller fragments. The fully swollen hydrogel was completely transparent.

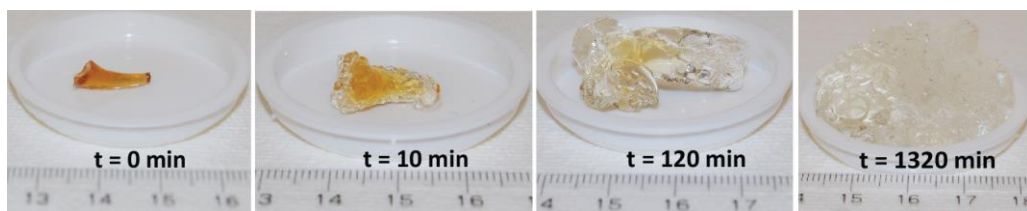


Figure 20. Swelling behaviour of [GGM5-MA0.14;20;10;5]; 0.150 g of the dried hydrogel was able to take up 10.4 mL of water.

Figure 21 illustrates typical SEM images of a fully swollen and consecutively freeze-dried GGM-based hydrogel ([GGM5-MA0.14;10;10;5]). The low-magnification image (Figure 21a) displays an overview of the sample and it could be observed that the hydrogel is present as unevenly shaped particles with a smooth surface. It has to be assumed that this surface morphology of the individual particles was formed during the freeze-drying process. Notably, after the drying process the cross-sectional area of broken particles reveals a highly porous structure (Figure 21b). The high amplification image (Figure 21c) features the extended surface of the material and led to the assumption that most of the quaternary ammonium groups are accessible for ion exchange in the swollen hydrogel.

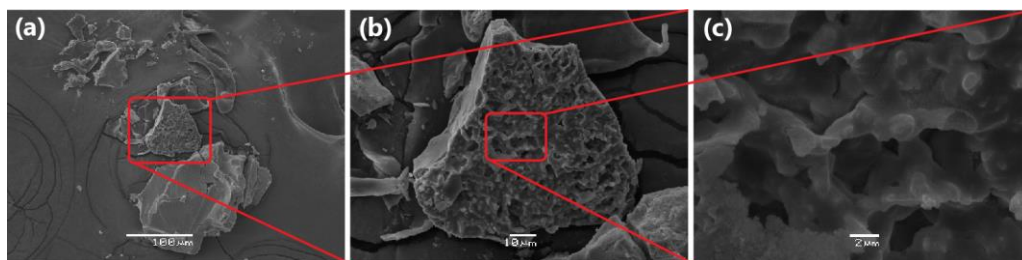


Figure 21. SEM images of a fully swollen GGM-based hydrogel ([GGM5-MA0.14;10;10;5]) after freeze-drying. The white bar represent 100 μm in a), 10 μm in b) and 2 μm in c).

It could be shown that GGM is a suitable starting material for the preparation of hydrogels with distinct swelling rates. Desired physical behaviour of the hydrogels can be tailored by choosing the right combination of the DS_{MA} of GGM, amount of monomer and initiator. Because the hydrogels contained cationic charges, they could be applied for the removal of metal ions for aqueous solutions by ion exchange (section 5.3.3).

5.3 Physical characterization and applications of the GGM derivatives

In order to analyse the physical properties of the synthesized GGM derivatives and to estimate their feasibility as novel bio-based products, different tests were performed. The GGM-*graft*-fatty acid and GGM-*block*-fatty acid, as well as the GGM-*block*-PDMS derivatives were studied with respect to their ability to lower the surface tension in water, as well as their application for the surface modification of NFC [I-III]. The GGM-based hydrogels were used as a sorbent material for the removal toxic arsenic and chromium ions from aqueous solutions. In the following abstracts the most important results are summarized.

5.3.1 Reduction of surface tension in water by GGM-fatty acid derivatives [I]

Detailed studies of the GGM-fatty acid derivatives in respect to their surface activity in water were performed. For this, solutions with different concentrations of GGM-*g*-C9 (0.80, 1.53, 2.23), GGM-*g*-C14 (0.82, 1.14, 1.95), and GGM-*g*-C18 (0.68, 1.07, 1.42), as well as the respective block-structured products of GGM and the fatty acids GGM-*b*-C9, GGM-*b*-C14, and GGM-*b*-C18, were prepared. The CAC values were determined by the break-points of the surface tension isotherms, which were estimated from the intersection of the fitted lines of the descending and flat part of the curves (Ferrer et al., 2002). For the products GGM-*g*-C14 (1.14), GGM-*g*-C18 (0.68), GGM-*g*-C18 (1.07), and GGM-*g*-C18 (1.42), the CAC could not be determined because the products were not

soluble at high concentrations (no plateau could be observed in the plots). For those products for which the CAC was possible to determine, the minimum surface tension γ_{\min} was determined and ranged between 44 and 57 mN/m. To understand the large differences between the minimum surface tensions, the surface excess Γ and the cross-sectional area per molecule A were calculated (see Table 5). The grafted- and the block-structured products needed to be evaluated separately. For GGM-g-C9 and GGM-g-C14, a higher degree of substitution led to a lower minimum surface tension and a simultaneous decrease of the cross-sectional area per molecule; however, the CAC is similar for the respective product series (same fatty acid). Considering one series of GGM-*graft*-fatty acid derivatives, the derivative with a higher degree of substitution was more surface active, presumably due to the presence of more hydrophobic chains located at the surface when forming a closely packed monolayer (Figure 22).

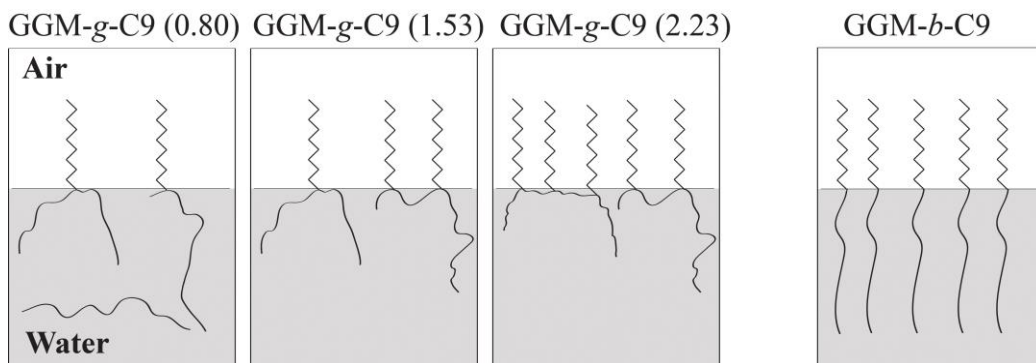


Figure 22. Schematic illustration of the GGM-*graft*-fatty acid (left) and GGM-*block*-fatty acid derivatives in water when the critical aggregation concentration (CAC) is reached.

The block-structured GGM-fatty acid derivatives were all soluble in water at high concentrations. The measured CAC values decreased from GGM-*b*-C9 to GGM-*b*-C18 while γ_{\min} increased. Taking the determined surface excess values into account, it can be assumed that for these products, not the GGM part but rather the hydrophobic chains are the limiting factor. This might be due to a denser packing of the short C9 chains at the surface compared to the longer C14 and C18 chains. The GGM chains are more flexible in the block-structured products and can arrange themselves in a more space-saving way compared to the grafted products. For the GGM derivatives of pelargonic acid (C9) and myristic acid (C14), the block-structured derivatives showed similar γ_{\min} values as the respective grafted products, with a FA/GGM ratio around 2. For the GGM-C18 derivatives, only the block-structured products had a sufficient solubility to show a significant surface activity.

Table 5. Properties of amphiphilic GGM derivatives in water. CAC is the critical aggregation concentration, γ_{\min} is the minimum surface tension determined, Γ represents the surface excess and A is the cross-sectional area per molecule.

Surfactant	CAC (mg/mL)	γ_{\min} (mN/m)	Γ (mol/m ²)	A (Å ²)
GGM	-	68.8	-	-
GGM-g-C9 (0.80)	1.28	55.0	1.5	111
GGM-g- C9 (1.53)	1.00	50.0	1.6	102
GGM-g- C9 (2.23)	1.22	44.4	1.7	99
GGM-g-C14 (0.82)	0.77	57.3	1.2	143
GGM-g-C14 (1.14)	ND ^a	<51.2	1.6	102
GGM-g-C14 (1.95)	0.78	51.1	1.8	94
GGM-g-C18 (0.68)	ND ^a	<56.8	1.4	117
GGM-g-C18 (1.07)	ND ^a	<61.3	0.8	214
GGM-g-C18 (1.42)	ND ^a	<61.0	0.9	175
GGM-b-C9	2.44	44.5	2.3	73
GGM-b-C14	1.82	47.11	1.4	111
GGM-b-C18	0.88	49.5	1.7	96

^a not determined

The results prove that it is possible to build amphiphilic GGM-fatty acid derivatives and encourage following up the research of fully bio-based surfactants.

5.3.2 Modification of cellulosic surfaces by amphiphilic GGM derivatives [III]

The synthesized GGM block-structured derivatives, in which a hydrophobic tail was attached to the GGM chain, were assumed to be a suitable material for the surface modification of cellulosic materials. Hereby the GGM chain could attach to the cellulose due to its high affinity to cellulose and the hydrophobic tail would accumulate on the cellulose surface increasing its overall hydrophobicity. The GGM block-structured derivatives were preferred for these experiments instead of the grafted derivatives, because in the grafted GGM derivatives the main chain of GGM was modified, what could reduce the affinity of GGM towards cellulose resulting in minor sorption. QCM-D was reported to be a well suitable method for the quantification of the adsorption of GGM on thin NFC films (Eronen et al., 2011). Hence QCM-D was used to analyse the sorption of selected GGM block-structured derivatives (GGM-*block*-C9, GGM-*block*-C14, GGM-*block*-C18 and GGM-*block*-PDMS). Therefore, firstly the crystal was coated

with a thin layer of NFC and consecutively a solution of native GGM and the distinguished GGM derivatives was brought in contact with the NFC surface (Figure 23).

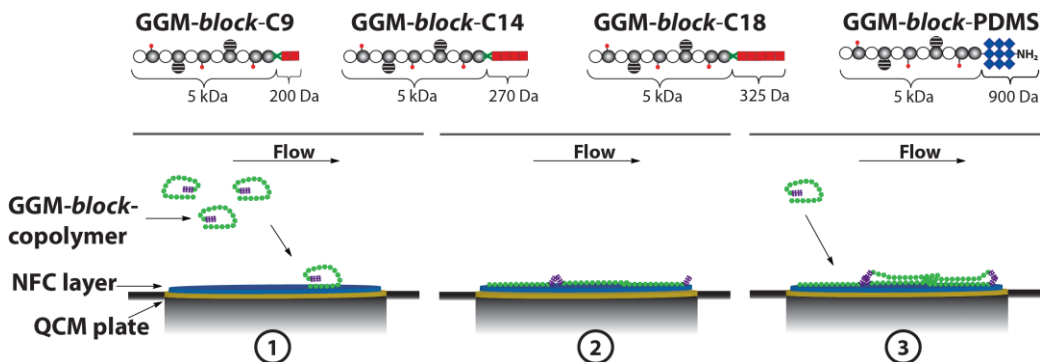


Figure 23. Molar mass and schematic structures of amphiphilic block-copolymers (GGM-b-C9, GGM-b-C14, GGM-b-C18, and GGM-b-PDMS). Schematic illustration of the possible change in conformation and build-up of a bilayer during adsorption of amphiphilic block-copolymers on NFC illustrated with GGM-b-PDMS on NFC surface. (1) Adsorption of the entangled GGM-b-PDMS on NFC; (2) formation of a viscoelastic layer; (3) build-up of bilayer.

While the GGM derivative solutions flowed over the crystal coated with NFC, first the formation of a monolayer was assumed where the GGM bound to the cellulose (2 in Figure 23). After the cellulose surface was fully covered with GGM, a second layer could build up while the hydrophobic tails agglomerated (3 in Figure 23). The adsorption of the GGM derivatives was followed by a change in frequency (Δf , 3rd overtone), which was plotted as a function of time (Figure 24).

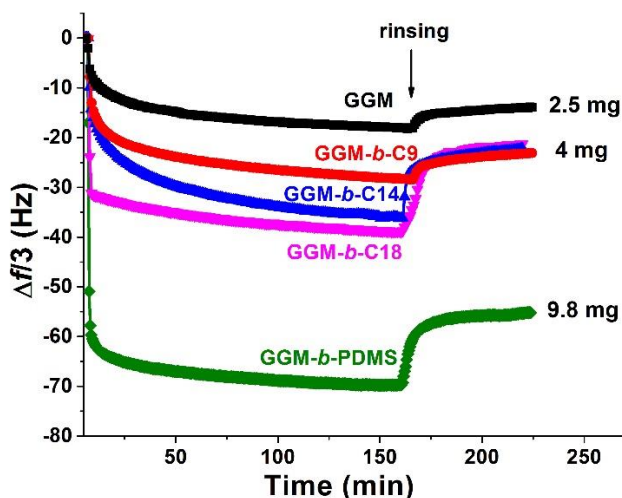


Figure 24. Results of the QCM-D experiments. Change in frequency (Δf_3) with time during adsorption of unmodified GGM, GGM-block-C9, GGM-block-C14, GGM-block-C18, or GGM-block-PDMS on NFC substrate from 0.5 g/L aqueous solutions. The polymer was injected at $t = 5$ min. Numbers on the graph indicate sensed adsorbed mass after rinsing.

After the adsorption was completed, the cellulose surface was rinsed with deionized water in order to remove all the molecules, which had not been strongly attached to the surface. The removal of loose molecules was accompanied by an increase in the frequency during the QCM-D measurement. The estimated sensed mass of each GGM derivative and native GGM adsorbed after rinsing was calculated and was 2.5 mg/m² for native GGM, around 4 mg/m² for the three GGM-block-fatty acids, and 9.8 mg/m² for the GGM-block-PDMS. The increased adsorption of the GGM-block-PDMS was ascribed to the high hydrophobicity of the PDMS chain, which was assumed to accelerate and increase its adsorption compared to the GGM-block-fatty acid derivatives containing shorter hydrophobic tails. The results of the QCM-D proved the adsorption of the GGM derivatives on NFC and the gained knowledge was used for the performance of further experiments. So NFC films were coated with the distinguished GGM derivatives by spin-coating and the produced films were analysed in respect of their oxygen permeability and contact angle. It was found that the oxygen permeability did not decrease significantly for the NFC film coated with the GGM derivatives, at 0 % and at 80 % relative humidity. Even though the decrease in the oxygen permeability was low, a trend that a larger effect on the decrease of the oxygen permeability the longer the hydrophobic tail of the GGM derivative was could be assigned. The contact angle

determined for the different films also did not show big differences for the GGM-*block*-fatty acid derivatives compared to uncoated NFC films. However, a considerable increase of the contact angle for the GGM-*block*-PDMS could be measured (30° for neat NFC and 60° for NFC coated with GGM-*block*-PDMS). The fatty acids are assumed to be too short as a tail in the amphiphilic GGM derivative or the sorbed amounts were too small for having an impact on the hydrophobicity of the NFC. Also it has to be noted that the droplets during the contact angle measurements were absorbed rather fast into the NFC film. Overall it can be concluded that amphiphilic GGM derivatives can be adsorbed on cellulose surfaces and has showed potential for the modification of NFC. In this respect, NFC films and foams have been produced in which GGM surfactants were added to the NFC suspension before the biocomposites formation. This approach allows an extensive mixing of NFC and the GGM derivatives resulting in a homogeneous distribution of the different components in the final products. Exhaustive efforts are currently undertaken in order to generate new NFC-GGM composites and to study their potential for the removal of metal ions from aqueous solutions.

5.3.3 Metal ion removal from aqueous solution using GGM-based hydrogels [IV]

The different GGM-based hydrogels contained cationic groups and were tested with respect to their potential to remove chromium (VI) and arsenic (V) anions from aqueous solutions (Paper [IV]) (ion species at different pH values can be found in Figure 27). In a first experiment set, five GGM-based hydrogels were applied for the ion removal and hereby revealed a high sorption potential (Figure 25).

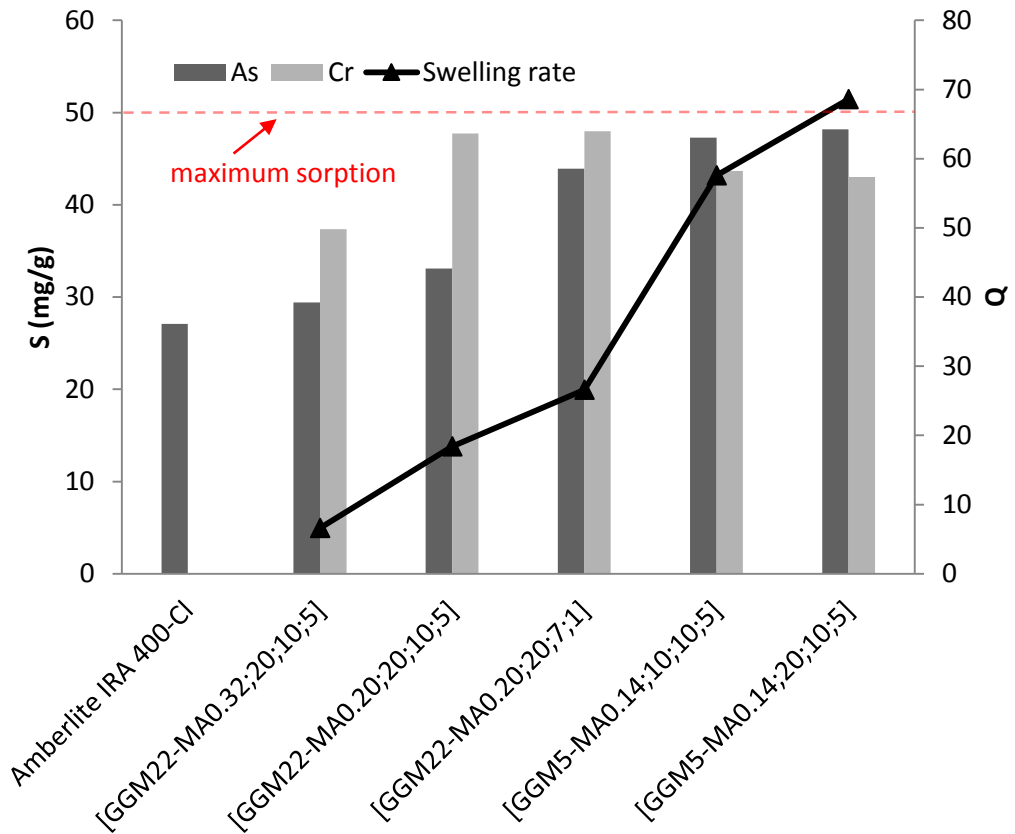


Figure 25. Sorption of As(V) and Cr(VI) for different hydrogels and Amberlite IRA 400-Cl as a commercial product. The maximum possible sorption in the experiments was 50 mg/g.

The experiments were performed at pH 9 to ensure that the ions of arsenic and chromium were present in their anionic form. In Figure 25, the sorption (S) as a function of the swelling rate (Q) of the hydrogels is shown. For As(V), a higher sorption was determined at an increasing swelling rate. This is assumed to be due to the increased amount of quaternary ammonium groups of the material available for ion exchange with arsenic oxy-anions due to the increased surface area inside the hydrogel. The maximum sorption was 48.17 mg As(V) sorbed per g of hydrogel (sample [GGM5-MAO.14;20;10;5]), what corresponds to 96 % of the ions present in the starting solution. The sorption capacities were considerably higher compared to commercial resins such as Amberlite IRA 400-Cl, for which a maximal sorption of 27.1 mg/g was determined at identical conditions (Rivas & Muñoz, 2009). The chromate ion sorption was higher than for the arsenic ions for low swelling rate and reached a maximum for the hydrogel

[GGM22-MA0.20;20;7;1]. In further preliminary experiments, the effect of the pH value on the sorption capacity was studied (Figure 26).

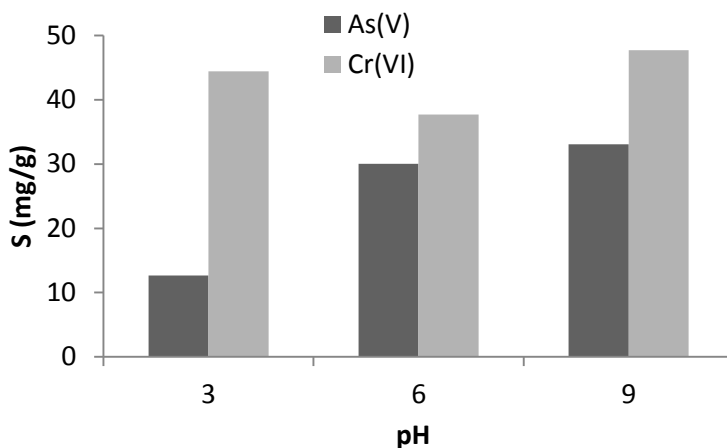


Figure 26. Sorption of As(V) and Cr(VI) as function of pH for the hydrogel [GGM22-MA0.20;20;10;5].

Arsenate revealed higher sorption at pH 6 and at pH 9 in comparison with pH 3. At pH 3, mostly the monovalent anionic species (H_2AsO_4^-) (Figure 27) is present and it is assumed that its lower charge density compared to HAsO_4^{2-} lead to a reduced ion exchange.

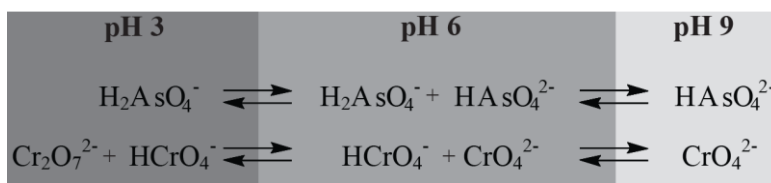


Figure 27. Ionic forms of arsenic and chromium species present at different pH values.

At pH 6, the monovalent (H_2AsO_4^-) and divalent (HAsO_4^{2-}) oxy-arsenic species exist in equilibrium (Sánchez et al., 2013) and the sorption increased compared to that at pH 3. The higher retention of As by the hydrogel at pH 9 can be attributed to the divalent species (see Figure 27). In the case of chromate, the highest retention capacity was reached at pH 9, where the divalent anionic CrO_4^{2-} species is predominant. The chromium removal was less efficient at pH 6 because CrO_4^{2-} and HCrO_4^- ions exist in equilibrium. At pH 3, the sorption was similar to that at pH 9 due to the presence of

$\text{Cr}_2\text{O}_7^{2-}$ ions. The sorption of chromate by the GGM-based hydrogel was high at a wide pH range, which could facilitate the application of the hydrogels for wastewater treatment.

In order to study the sorption capacity of the hydrogel, [GGM22-MA0.20;20;7;1] was used in successive batches (detailed conditions described in the experimental part).

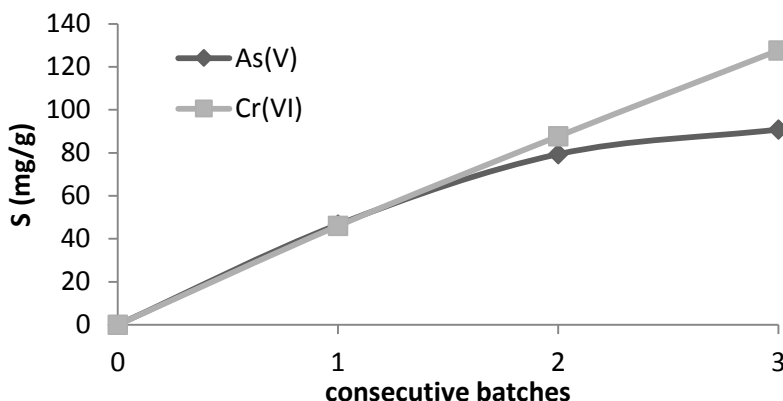


Figure 28. Sorption of As(V) and Cr(VI) in function of successive batches using [GGM22-MA0.20;20;7;1].

The results are shown in Figure 28 and after the first batch, a similar S value for As(V) and Cr(VI) (around 40 mg/g) was determined. After that, the loaded hydrogel was submitted to a second batch (solution 100 mg/L of As(V) resp. Cr(VI)). The results showed that the hydrogel could remove similar amounts of ions as for the first batch reaching values around 80 mg/g. In a consecutively performed third batch, it could be observed that the hydrogel still removed the chromate ions in a constant rate compared to the two first batches, reaching a maximum value of $S = 127$ mg/g. However, in the case of the arsenic ions a reduced up-take capacity for the third batch was assessed, indicating saturation of the active groups in the hydrogels.

Overall it was found that the GGM-based hydrogels have a high potential for the purification of wastewaters and more detailed studies will be carried out in order to tailor the physical properties of the GGM-based hydrogels.

6. CONCLUDING REMARKS

In this work the chemical modification of *O*-acetyl galactoglucomannan (GGM) and the potential applications of the GGM derivatives were studied. The experiments were performed using GGM with a number-average molar mass of 5 and 22 kDa with a relatively narrow molar mass distribution. In the performed reactions the hydroxyl groups were targeted and converted in either esterification or transesterification reactions. Furthermore, the reducing end of GGM was modified by reductive amination resulting in well-defined block-structured derivatives.

In a first reaction set, GGM was reacted with different activated fatty acids in an esterification giving GGM-grafted-fatty acid derivatives with DS-values ranging between 0.03 and 0.17. The GGM-*graft*-fatty acids showed a tendency being less water-soluble when the longer the respective fatty acid chain was and the higher the DS value was. Besides the grafted GGM-fatty acid derivatives, also GGM block-structured products were synthesized. Hereby, an amino-functional fatty acid was converted in a reductive amination with the reducing end of GGM. For the experiment, three different fatty acids (C9, C14, and C18) were applied and the resulting block-structured derivatives were all readily soluble in water. Due to their amphiphilic structure and the simultaneous solubility even at higher concentrations, the products were tested in respect to their ability to reduce the surface tension of water. The measurements showed a minimal surface tension of 46 to 50 mN/m; the GGM-fatty acid derivative with the smallest fatty acid was more effective.

The GGM-block-fatty acids were together with a block-structured GGM-PDMS derivative tested in respect to their potential to be used as an additive for the hydrophobization of cellulosic surfaces. Therefore, QCM-D experiments were carried out and the sorption of the respective derivative ranged from 4.0 to 9.8 mg/m² cellulose surface area. Hereby, it was assumed that the GGM derivatives are forming double layers and the GGM-block-PDMS derivative yields a higher sorption amount because of its higher hydrophobicity and higher molar mass than other fatty acid derivatives. The contact angle of NFC films coated with the GGM derivatives was measured and it was found that the hydrophobicity of the film could be increased and as expected were highest for GGM-block-PDMS. The experiments showed that GGM is a potential carrier of functional groups which can be applied in the modification of NFC surface.

The application of fatty acids for the synthesis of GGM block-structured derivatives has the limitation that the chain length of the hydrophobic tail is restricted by the initially

used fatty acid. In order to be able to design novel GGM derivatives in which the synthetic tail has flexible molar mass and distinguished physicochemical properties, synthesis paths including a controlled polymerization was developed. Therefore, a beforehand amino-functional initiator was converted with the reducing end followed by single electron transfer-living radical polymerization. The obtained GGM block-structured derivatives feature a synthetic polymer chain at the reducing end with a defined molar mass and were either hydrophobic, charged or temperature- and pH-sensitive. The acquired results demonstrated the possibility to produce well-defined GGM block-structured derivatives with determined functionalities.

In a further experimental approach, GGM macromonomers were synthesized by transesterification and GGM macromonomers with different DS values were obtained, purified and well characterized. The different GGM macromonomers were further applied as crosslinkers in the production of cationic hydrogels. The physical properties of the hydrogels were tailored by used defined amounts of monomers, initiator and the respective GGM macromonomer. For all the produced hydrogels the swelling rates were determined and tested in respect to their ability to remove toxic Cr and As ions from aqueous solutions. It was found that the GGM-based hydrogels reveal a high potential to remove anions from contaminated water and the results are highly encouraging to carry out more detailed research.

Overall this work underlines the urge to continue innovative research in the area of renewable materials, especially in order to use the plant hemicelluloses, which are nowadays still eliminated in a large amount in the industry. The high potential for a large scale application of plant materials in everyday goods is given and scientists will soon be able to offer the needed tools and economical plan for its realization.

NOTATIONS

AIBN	azobisisobutyronitrile
ATRP	atom transfer radical polymerization
BIBB	α -bromoisobutyryl bromide
CA	contact angle
CAC	critical aggregation concentrations
CDI	1,1'-carbonyldiimidazole
CMC	critical micelle concentration
Da	Dalton
DMAP	4-(dimethylamino)pyridine
DMF	dimethylformamide
DMSO	dimethyl sulfoxide
DS	degree of substitution
DS _{Ac}	degree of acetylation
DSC-TGA	differential scanning calorimetry-thermal gravimetric analysis
Et ₃ N	triethylamine
EtOH	ethanol
FTIR	fourier transformed infrared spectroscopy
Gal	galactose
GGM	O-acetyl galactoglucomannan
Glc	glucose
GMA	glycidyl methacrylate
HPSEC	high performance size exclusion chromatography
Man	mannose
MeDMA	[2-(methacryloyloxy)ethyl]trimethylammonium chloride
MeOH	methanol
MMA	methyl methacrylate
M _n	number-average molar mass
MTBE	methyl tert-butyl ether
M _w	weight-average molar mass
N _A	Avogadro's number
NFC	nanofibrillated cellulose
NH ₂ -PDMS-NH ₂	bis(3-aminopropyl) terminated poly(dimethylsiloxane)
NIPAM	N-isopropylacrylamide
NMR	nuclear magnetic resonance spectroscopy
OTR	oxygen transmission rate

PDI	polydispersity index
Q	swelling ratio
QCM-D	quartz crystal microbalance with dissipation
R	ideal gas constant
RAFT	reversible addition-fragmentation chain transfer
ROP	ring opening polymerization
SEM	scanning electron microscopy
SET-LRP	single electron transfer-living radical polymerization
T	absolute temperature
TEMPO	(2,2,6,6-tetramethylpiperidin-1-yl)oxy
TFA	trifluoroacetic acid
THF	tetrahydrofuran
Γ	surface excess

REFERENCES

- Al Manasrah, M., Kallioinen, M., Ilvesniemi, H., Mänttari, M. 2012. Recovery of galactoglucomannan from wood hydrolysate using regenerated cellulose ultrafiltration membranes. *Bioresource Technology*, **114**, 375-81.
- Albertsson, A.-C., Voepel, J., Edlund, U., Dahlman, O., Söderqvist-Lindblad, M. 2010. Design of Renewable Hydrogel Release Systems from Fiberboard Mill Wastewater. *Biomacromolecules*, **11**(1406-1411), 1406.
- Andresen, M., Stenius, P. 2007. Water - in - oil Emulsions Stabilized by Hydrophobized Microfibrillated Cellulose. *Journal of Dispersion Science and Technology*, **28**(6), 837-844.
- Ayoub, A., Venditti, R.A., Pawlak, J.J., Salam, A., Hubbe, M.A. 2013. Novel Hemicellulose–Chitosan Biosorbent for Water Desalination and Heavy Metal Removal. *ACS Sustainable Chemistry & Engineering*, **1**(9), 1102-1109.
- Bernard, J., Save, M., Arathoon, B., Charleux, B. 2008. Preparation of a xanthate-terminated dextran by click chemistry: Application to the synthesis of polysaccharide-coated nanoparticles via surfactant-free ab initio emulsion polymerization of vinyl acetate. *Journal of Polymer Science Part A: Polymer Chemistry*, **46**(8), 2845-2857.
- Bosker, W.T.E., Ágoston, K., Cohen Stuart, M.A., Norde, W., Timmermans, J.W., Slaghek, T.M. 2003. Synthesis and Interfacial Behavior of Polystyrene–Polysaccharide Diblock Copolymers. *Macromolecules*, **36**(6), 1982-1987.
- Bütün, V., Liu, S., Weaver, J.V.M., Bories-Azeau, X., Cai, Y., Armes, S.P. 2006. A brief review of ‘schizophrenic’ block copolymers. *Reactive and Functional Polymers*, **66**(1), 157-165.
- Cai, D., Neyer, A., Kuckuk, R., Heise, H.M. 2010. Raman, mid-infrared, near-infrared and ultraviolet–visible spectroscopy of PDMS silicone rubber for

- characterization of polymer optical waveguide materials. *Journal of Molecular Structure*, **976**, 274-281.
- Capek, P., Kubačková, M., Alföldi, J., Bilisics, L., Lišková, D., Kákoniová, D. 2000. Galactoglucomannan from the secondary cell wall of *Picea abies* L. Karst. *Carbohydrate Research*, **329**(3), 635-645.
- Ciampolini, M., Nardi, N. 1966. Five-Coordinated High-Spin Complexes of Bivalent Cobalt, Nickel, and Copper with Tris(2-dimethylaminoethyl)amine. *Inorganic Chemistry*, **5**(1), 41-44.
- Cushen, J.D., Otsuka, I., Bates, C.M., Halila, S., Fort, S., Rochas, C., Easley, J.A., Rausch, E.L., Thio, A., Borsali, R., Willson, C.G., Ellison, C.J. 2012. Oligosaccharide/Silicon-Containing Block Copolymers with 5 nm Features for Lithographic Applications. *ACS Nano*, **6**(4), 3424-3433.
- Davis, N.J., Flitsch, S.L. 1993. Selective oxidation of monosaccharide derivatives to uronic acids. *Tetrahedron Letters*, **34**(7), 1181-1184.
- de Nooy, A.E.J., Besemer, A.C., van Bekkum, H. 1995. Highly selective nitroxyl radical-mediated oxidation of primary alcohol groups in water-soluble glucans. *Carbohydrate Research*, **269**(1), 89-98.
- Edlund, U., Albertsson, A.-C. 2012. SET-LRP goes “green”: Various hemicellulose initiating systems under non-inert conditions. *Journal of Polymer Science Part A: Polymer Chemistry*, **50**(13), 2650-2658.
- Elkins, C.L., Long, T.E. 2004. Living Anionic Polymerization of Hexamethylcyclotrisiloxane (D3) Using Functionalized Initiation. *Macromolecules*, **37**(17), 6657-6659.
- Enomoto-Rogers, Y., Iwata, T. 2012. Synthesis of xylan-graft-poly(l-lactide) copolymers via click chemistry and their thermal properties. *Carbohydrate Polymers*, **87**(3), 1933-1940.

- Eronen, P., Österberg, M., Heikkinen, S., Tenkanen, M., Laine, J. 2011. Interactions of structurally different hemicelluloses with nanofibrillar cellulose. *Carbohydrate Polymers*, **86**(3), 1281-1290.
- Ferrer, M., Comelles, F., Plou, F.J., Cruces, M.A., Fuentes, G., Parra, J.L., Ballesteros, A. 2002. Comparative Surface Activities of Di- and Trisaccharide Fatty Acid Esters. *Langmuir*, **18**(3), 667-673.
- Fleischmann, S., Rosen, B.M., Percec, V. 2010. SET-LRP of acrylates in air. *Journal of Polymer Science Part A: Polymer Chemistry*, **48**(5), 1190-1196.
- Fundador, N.G.V., Enomoto-Rogers, Y., Takemura, A., Iwata, T. 2012. Syntheses and characterization of xylan esters. *Polymer*, **53**(18), 3885-3893.
- Goussé, C., Chanzy, H., Cerrada, M.L., Fleury, E. 2004. Surface silylation of cellulose microfibrils: preparation and rheological properties. *Polymer*, **45**(5), 1569-1575.
- Grefte, L., Bessueille, L., Bulone, V., Brumer, H. 2005. Synthesis, preliminary characterization, and application of novel surfactants from highly branched xyloglucan oligosaccharides. *Glycobiology*, **15**(4), 437-45.
- Grote, C., Heinze, T. 2005. Starch Derivatives of High Degree of Functionalization 11: Studies on Alternative Acylation of Starch with Long-chain Fatty Acids Homogeneously in N,N-dimethyl acetamide/LiCl. *Cellulose*, **12**(4), 435-444.
- Haddleton, D.M., Ohno, K. 2000. Well-Defined Oligosaccharide-Terminated Polymers from Living Radical Polymerization. *Biomacromolecules*, **1**(2), 152-156.
- Halila, S., Manguian, M., Fort, S., Cottaz, S., Hamaide, T., Fleury, E., Driguez, H. 2008. Syntheses of Well-Defined Glyco-Polyorganosiloxanes by “Click” Chemistry and their Surfactant Properties. *Macromolecular Chemistry and Physics*, **209**(12), 1282-1290.

- Hannuksela, T., Hervé du Penhoat, C. 2004. NMR structural determination of dissolved O-acetylated galactoglucomannan isolated from spruce thermomechanical pulp. *Carbohydrate Research*, **339**(2), 301-312.
- Hansen, N.M.L., Plackett, D. 2008. Sustainable Films and Coatings from Hemicelluloses: A Review. *Biomacromolecules*, **9**(6), 1493-1505.
- Harihara Subramanian, S., Prakash Babu, R., Dhamodharan, R. 2008. Ambient Temperature Polymerization of Styrene by Single Electron Transfer Initiation, Followed by Reversible Addition Fragmentation Chain Transfer Control. *Macromolecules*, **41**, 262-265.
- Hartman, J., Albertsson, A.-C., Lindblad, M.S., Sjöberg, J. 2006a. Oxygen barrier materials from renewable sources: Material properties of softwood hemicellulose-based films. *Journal of Applied Polymer Science*, **100**(4), 2985-2991.
- Hartman, J., Albertsson, A.-C., Sjöberg, J. 2006b. Surface- and Bulk-Modified Galactoglucomannan Hemicellulose Films and Film Laminates for Versatile Oxygen Barriers. *Biomacromolecules*, **7**(6), 1983-1989.
- Heikkinen, S.L., Mikkonen, K.S., Koivisto, P., Heikkilä, M.I., Pirkkalainen, K., Liljeström, V., Serimaa, R., Tenkanen, M. 2013. Long-Term Physical Stability of Plasticized Hemicellulose Films. *Bioresources*, **9**(1), 906-921.
- Heinze, T., Liebert, T., Koschella, A. 2006. *Esterification of Polysaccharides*. Springer Berlin Heidelberg.
- Hernandez, O.S., Soliman, G.M., Winnik, F.M. 2007. Synthesis, reactivity, and pH-responsive assembly of new double hydrophilic block copolymers of carboxymethyldextran and poly(ethylene glycol). *Polymer*, **48**(4), 921-930.
- Höök, F., Kasemo, B., Nylander, T., Fant, C., Sott, K., Elwing, H. 2001. Variations in Coupled Water, Viscoelastic Properties, and Film Thickness of a Mefp-1 Protein Film during Adsorption and Cross-Linking: A Quartz Crystal Microbalance

with Dissipation Monitoring, Ellipsometry, and Surface Plasmon Resonance Study. *Analytical Chemistry*, **73**(24), 5796-5804.

Houga, C., Giermanska, J., Lecommandoux, S., Borsali, R., Taton, D., Gnanou, Y., Le Meins, J.-F. 2008. Micelles and Polymersomes Obtained by Self-Assembly of Dextran and Polystyrene Based Block Copolymers. *Biomacromolecules*, **10**(1), 32-40.

Houga, C., Le Meins, J.F., Borsali, R., Taton, D., Gnanou, Y. 2007. Synthesis of ATRP-induced dextran-b-polystyrene diblock copolymers and preliminary investigation of their self-assembly in water. *Chem Commun (Camb)*(29), 3063-5.

Hubbe, M.A., Rojas, O.J., Lucia, L.A., Sain, M. 2008. Cellulosic nanocomposites: A review. *Bioresources*, **3**(3), 929-980.

Hussain, M.A., Liebert, T., Heinze, T. 2004. Acylation of Cellulose with N,N' - Carbonyldiimidazole-Activated Acids in the Novel Solvent Dimethyl Sulfoxide/Tetrabutylammonium Fluoride. *Macromolecular Rapid Communications*, **25**(9), 916-920.

Jönsson, B., Lindman, B., Holmberg, K., Kronberg, B. 1998. Surfactants and Polymers in Aqueous Solutions, Wiley. West Sussex.

Kilpeläinen, P., Kitunen, V., Pranovich, A., Iivesmiemi, Willför, S. 2013. Pressurized hot water flow-through extraction of birch sawdust with acetate pH buffer. *Bioresources*, **8**(4), 5202-5218.

Kisonen, V., Eklund, P., Auer, M., Sjöholm, R., Pranovich, A., Hemming, J., Sundberg, A., Aseyev, V., Willför, S. 2012. Hydrophobication and characterisation of O-acetyl-galactoglucomannan for papermaking and barrier applications. *Carbohydrate Research*, **352**, 151-8.

- Klemm, D., Heublein, B., Fink, H.P., Bohn, A. 2005. Cellulose: fascinating biopolymer and sustainable raw material. *Angewandte Chemie (International ed. in English)*, **44**(22), 3358-3393.
- Kochumalayil, J.J., Zhou, Q., Kasai, W., Berglund, L.A. 2013. Regioselective modification of a xyloglucan hemicellulose for high-performance biopolymer barrier films. *Carbohydrate Polymers*, **93**(2), 466-472.
- Kongruang, S., Penner, M.H. 2004. Borohydride reactivity of cellulose reducing ends. *Carbohydrate Polymers*, **58**(2), 131-138.
- Leppänen, A.-S., Xu, C., Eklund, P., Lucenius, J., Österberg, M., Willför, S. 2013. Targeted functionalization of spruce O-acetyl galactoglucomannans-2,2,6,6-tetramethylpiperidin-1-oxyl-oxidation and carbodiimide-mediated amidation. *Journal of Applied Polymer Science*, **130**(5), 3122-3129.
- Li, B.-G., Zhang, L.-M. 2008. Synthesis and characterization of novel amphiphilic block copolymers based on maltoheptaose and poly(ϵ -caprolactone). *Carbohydrate Polymers*, **74**(3), 390-395.
- Liu, J.-Y., Zhang, L.-M. 2007. Preparation of a polysaccharide–polyester diblock copolymer and its micellar characteristics. *Carbohydrate Polymers*, **69**(1), 196-201.
- Loos, K., Stadler, R. 1997. Synthesis of Amylose-block-polystyrene Rod–Coil Block Copolymers. *Macromolecules*, **30**(24), 7641-7643.
- Michielsen, S., Brandrup, J., Immergut, E.H. 1999. *Polymer Handbook. 4 ed.* Wiley, New York.
- Missoum, K., Belgacem, M., Bras, J. 2013. Nanofibrillated Cellulose Surface Modification: A Review. *Materials*, **6**(5), 1745-1766.

- Nakagaito, A.N., Yano, H. 2004. The effect of morphological changes from pulp fiber towards nano-scale fibrillated cellulose on the mechanical properties of high-strength plant fiber based composites. *Applied Physics A*, **78**(4), 547-552.
- Pääkkö, M., Ankerfors, M., Kosonen, H., Nykänen, A., Ahola, S., Österberg, M., Ruokolainen, J., Laine, J., Larsson, P.T., Ikkala, O., Lindström, T. 2007. Enzymatic Hydrolysis Combined with Mechanical Shearing and High-Pressure Homogenization for Nanoscale Cellulose Fibrils and Strong Gels. *Biomacromolecules*, **8**(6), 1934-1941.
- Parikka, K., Leppänen, A.-S., Pitkänen, L., Reunanen, M., Willför, S., Tenkanen, M. 2009. Oxidation of Polysaccharides by Galactose Oxidase. *Journal of Agricultural and Food Chemistry*, **58**(1), 262-271.
- Peng, X.-W., Ren, J.-L., Zhong, L.-X., Peng, F., Sun, R.-C. 2011. Xylan-rich Hemicelluloses-graft-Acrylic Acid Ionic Hydrogels with Rapid Responses to pH, Salt, and Organic Solvents. *Journal of Agricultural and Food Chemistry*, **59**(15), 8208-8215.
- Peng, X., Ren, J., Zhong, L., Sun, R., Shi, W., Hu, B. 2012a. Glycidyl methacrylate derivatized xylan-rich hemicelluloses: synthesis and characterizations. *Cellulose*, **19**(4), 1361-1372.
- Peng, X.W., Zhong, L.X., Ren, J.L., Sun, R.C. 2012b. Highly effective adsorption of heavy metal ions from aqueous solutions by macroporous xylan-rich hemicelluloses-based hydrogel. *J Agric Food Chem*, **60**(15), 3909-16.
- Percec, V., Popov, A.V., Ramirez-Castillo, E., Monteiro, M., Barboiu, B., Weichold, O., Asandei, A.D., Mitchell, C.M. 2002. Aqueous Room Temperature Metal-Catalyzed Living Radical Polymerization of Vinyl Chloride. *Journal of the American Chemical Society*, **124**(18), 4940-4941.
- Prabaharan, M., Mano, J.F. 2006. Stimuli-responsive hydrogels based on polysaccharides incorporated with thermo-responsive polymers as novel biomaterials. *Macromol Biosci*, **6**(12), 991-1008.

- Prado, H.J., Matulewicz, M.C. 2014. Cationization of polysaccharides: A path to greener derivatives with many industrial applications. *European Polymer Journal*, **52**(0), 53-75.
- Rivas, B.L., Muñoz, C. 2009. Functional water-insoluble polymers with ability to remove arsenic(V). *Polymer Bulletin*, **65**(1), 1-11.
- Roos, A.A., Edlund, U., Sjöberg, J., Albertsson, A.-C., Stålbrand, H. 2008. Protein Release from Galactoglucomannan Hydrogels: Influence of Substitutions and Enzymatic Hydrolysis by β -Mannanase. *Biomacromolecules*, **9**(8), 2104-2110.
- Sá-Lima, H., Caridade, S.G., Mano, J.F., Reis, R.L. 2010. Stimuli-responsive chitosan-starch injectable hydrogels combined with encapsulated adipose-derived stromal cells for articular cartilage regeneration. *Soft Matter*, **6**(20), 5184.
- Sadhu, V.B., Pionteck, J., Voigt, D., Komber, H., Voit, B. 2004. Synthesis of halogen-free amino-functionalized polymethyl methacrylate by atom transfer radical polymerization(ATRP). *Macromolecular Symposia*, **210**(1), 147-155.
- Saito, T., Nishiyama, Y., Putaux, J.-L., Vignon, M., Isogai, A. 2006. Homogeneous Suspensions of Individualized Microfibrils from TEMPO-Catalyzed Oxidation of Native Cellulose. *Biomacromolecules*, **7**(6), 1687-1691.
- Sánchez, J., Bastrzyk, A., Rivas, B.L., Bryjak, M., Kabay, N. 2013. Removal of As(V) using liquid-phase polymer-based retention (LPR) technique with regenerated cellulose membrane as a filter. *Polymer Bulletin*, **70**(9), 2633-2644.
- Sauerbrey, G. 1959. Verwendung von Schwingquarzen zur Wägung dünner Schichten und zur Mikrowägung. *Zeitschrift für Physik*, **155**(2), 206-222.
- Schatz, C., Lecommandoux, S. 2010. Polysaccharide-Containing Block Copolymers: Synthesis, Properties and Applications of an Emerging Family of Glycoconjugates. *Macromolecular Rapid Communications*, **31**(19), 1664-1684.

- Sehaqui, H., Zhou, Q., Berglund, L.A. 2011. High-porosity aerogels of high specific surface area prepared from nanofibrillated cellulose (NFC). *Composites Science and Technology*, **71**(13), 1593-1599.
- Sehaqui, H., Zimmermann, T., Tingaut, P. 2014. Hydrophobic cellulose nanopaper through a mild esterification procedure. *Cellulose*, **21**(1), 367-382.
- Sjöström, E. 1993. *Wood Chemistry - Fundamentals and Applications*. Academic Press, San Diego, USA.
- Song, T., Pranovich, A., Sumerskiy, I., Holmbom, B. 2008. Extraction of galactoglucomannan from spruce wood with pressurised hot water. *Holzforschung*, **62**(6), 659-666.
- Suriano, F., Pratt, R., Tan, J.P., Wiradharma, N., Nelson, A., Yang, Y.Y., Dubois, P., Hedrick, J.L. 2010. Synthesis of a family of amphiphilic glycopolymers via controlled ring-opening polymerization of functionalized cyclic carbonates and their application in drug delivery. *Biomaterials*, **31**(9), 2637-45.
- Svagan, A.J., Azizi Samir, M.A.S., Berglund, L.A. 2007. Biomimetic Polysaccharide Nanocomposites of High Cellulose Content and High Toughness. *Biomacromolecules*, **8**, 2556-2563.
- Timell, T.E. 1982. Recent progress in the chemistry and topochemistry of compression wood. *Wood Science and Technology*, **16**(2), 83-122.
- Vaca-Garcia, C., Thiebaud, S., Borredon, M.E., Gozzelino, G. 1998. Cellulose esterification with fatty acids and acetic anhydride in lithium chloride/N,N-dimethylacetamide medium. *Journal of the American Oil Chemists' Society*, **75**(2), 315-319.
- Vashist, A., Vashist, A., Gupta, Y.K., Ahmad, S. 2014. Recent advances in hydrogel based drug delivery systems for the human body. *Journal of Materials Chemistry B*, **2**(2), 147-166.

- Voepel, J., Edlund, U., Albertsson, A.-C. 2011a. A versatile single-electron-transfer mediated living radical polymerization route to galactoglucomannan graft-copolymers with tunable hydrophilicity. *Journal of Polymer Science Part A: Polymer Chemistry*, **49**(11), 2366-2372.
- Voepel, J., Edlund, U., Albertsson, A.-C., Percec, V. 2011b. Hemicellulose-Based Multifunctional Macroinitiator for Single-Electron-Transfer Mediated Living Radical Polymerization. *Biomacromolecules*, **12**, 253-259.
- Willför, S., Sjöholm, R., Laine, C., Roslund, M., Hemming, J., Holmbom, B. 2003. Characterisation of water-soluble galactoglucomannans from Norway spruce wood and thermomechanical pulp. *Carbohydrate Polymers*, **52**, 175-187.
- Willför, S., Sundberg, K., Tenkanen, M., Holmbom, B. 2008. Spruce-derived mannans – A potential raw material for hydrocolloids and novel advanced natural materials. *Carbohydrate Polymers*, **72**(2), 197-210.
- Xu, C., Spadiut, O., Araújo, A.C., Nakhai, A., Brumer, H. 2012. Chemo-enzymatic Assembly of Clickable Cellulose Surfaces via Multivalent Polysaccharides. *ChemSusChem*, **5**(4), 661-665.
- Yamanaka, S., Watanabe, K., Kitamura, N. 1989. The structure and mechanical properties of sheets prepared from bacterial cellulose. *Journal of Materials Science*, **24**, 3141-3145.
- Zhang, T., Marchant, R.E. 1994. Novel Polysaccharide Surfactants: Synthesis of Model Compounds and Dextran-Based Surfactants. *Macromolecules*, **27**(25), 7302-7308.
- Zhang, X., Lin, W., Chen, S., Xu, H., Gu, H. 2011. Development of a stable dual functional coating with low non-specific protein adsorption and high sensitivity for new superparamagnetic nanospheres. *Langmuir*, **27**(22), 13669-74.

- Zheng, Y., Wang, W., Zhu, G., Wang, A. 2013. Enhanced Selectivity for Heavy Metals Using Polyaniline-Modified Hydrogel. *Industrial & Engineering Chemistry Research*, **52**(13), 4957-4961.
- Zhong, L.-X., Peng, X.-W., Yang, D., Cao, X.-F., Sun, R.-C. 2012. Long-Chain Anhydride Modification: A New Strategy for Preparing Xylan Films. *Journal of Agricultural and Food Chemistry*, **61**(3), 655-661.
- Zoppe, J.O., Habibi, Y., Rojas, O.J., Venditti, R.A., Johansson, L.-S., Efimenko, K., Österberg, M., Laine, J. 2010. Poly(N-isopropylacrylamide) Brushes Grafted from Cellulose Nanocrystals via Surface-Initiated Single-Electron Transfer Living Radical Polymerization. *Biomacromolecules*, **11**, 2683-2691.



BIOREGS

polysaccharides for a sweet future

ISBN 978-952-12-3115-5
Painosalama Oy – Turku, Finland 2014